ARMY RESEARCH LABORATORY

Experimental Validation of a Closed-Form Fluid Flow Model for Vacuum-Assisted Resin-Transfer Molding

by Bruce K. Fink, Roopesh Mathur, Dirk Heider, Christian Hoffman, John W. Gillespie, Jr., and Suresh G. Advani

ARL-TR-2495

May 2001

Army Research Laboratory

Aberdeen Proving Ground, MD 21005-5069

ARL-TR-2495 **May 2001**

Experimental Validation of a Closed-Form Fluid Flow Model for Vacuum-Assisted Resin-Transfer Molding

Bruce K. Fink
Weapons and Materials Research Directorate, ARL

Roopesh Mathur, Dirk Heider, Christian Hoffman,
John W. Gillespie, Jr., and Suresh G. Advani
University of Delaware

Abstract

Through-thickness measurements were recorded to experimentally investigate the through-thickness flow and to validate a closed-form solution of the resin flow during the vacuum-assisted resin-transfer molding (VARTM) process. During the VARTM process, a highly permeable distribution medium is incorporated into the preform as a surface layer, and resin is infused into the mold, under vacuum. During infusion, the resin flows preferentially across the surface and simultaneously through the thickness of the preform, giving rise to a three-dimensional flow front. The time to fill the mold and the shape of the flow front are critical for the optimal manufacture of large composite parts. An analytical model predicts the flow times and flow-front shapes as a function of the properties of the preform, distribution media, and resin. It was found that the flow-front profile reaches a steady state shape that is parabolic in shape and the length of the region saturated by resin is proportional to the square root of the time elapsed. Experimental measurements of the flow front in the process were carried out using embedded sensors to detect the flow of resin through the thickness of the preform layer and the progression of flow along the length of the part. The time to fill the part, the length of flow front, and its shape show good agreement between experiments and the analytical model. The experimental study demonstrates the need for control and optimization of resin injection during the manufacture of large parts by VARTM.

Contents

List of Figures v

List of Tables vii

1. Introduction 1

2. VARTM Process Modeling 3

3. Review of Analytical Model 4

4. VARTM Test Bed: Description of the Experimental Setup 7

5. Experimental Procedures 10
   - 5.1 3-D Preform Permeabilities 10
   - 5.2 Permeability of Distribution Medium 11
   - 5.3 Porosities of Fiber Preforms and Distribution Media 11
   - 5.4 Flow Experiments With Varying Preform Thickness 11

6. Conclusions 20

7. References 21

Distribution List 23

Report Documentation Page 41

INTENTIONALLY LEFT BLANK.

List of Figures

Figure 1. Schematic of the VARTM process. 2

Figure 2. Schematic and nomenclature used for the analytical model. 4

Figure 3. Mass conservation at the flow front. 5

Figure 4. Nominalized flow-front shapes for different number of layers (N) of fiber preforms. 8

Figure 5. Variation in the length of flow-front region (d) with preform thickness, predicted by the analytical model, for different values of permeability of the distribution medium (a typical permeability value for the distribution medium is 7.05E−05). 8

Figure 6. The UD-CCM VARTM workcell that incorporates sensors and enables flow model validation and VARTM automation. 9

Figure 7. Experimental SMARTweave grid with 21 excitation and 6 sense lines for the 15-layer E-glass preform. 12

Figure 8. Resin arrival time of 5-layer 411-C50 injection 85cP, 40 in × 6 in. 14

Figure 9. Resin arrival time of 9-layer 411-C50 injection 85cP, 40 in × 6 in. 14

Figure 10. Resin arrival time of 15-layer 411-C50 injection 85cP, 40 in × 6 in. 15

Figure 11. Resin arrival time of 30-layer 411-C50 injection 85cP, 40 in × 6 in. 15

Figure 12. Resin arrival time of 40-layer 411-C50 injection 85cP, 40 in × 6 in. 16

Figure 13. Arrival time of resin at the bottom layer: comparison of model prediction and experimental data from SMARTweave. 16

Figure 14. Reconstructed flow fronts from resin arrival data (a) 5 layers of preform material, (b) 9 layers of preform material, and (c) 15 layers of preform material. 17

Figure 15. Reconstructed flow fronts from resin arrival data (d) 30 layers of preform and (e) 40 layers of preform. 17

Figure 16. Length of flow region: comparison of model prediction with experimental observations for different number of layers of front-fiber preform. 18

Figure 17. Flow-front profile through the thickness: comparison of model predictions with experimental data for different number of layers of fiber preform. 19

INTENTIONALLY LEFT BLANK.

List of Tables

Table 1. Nomenclature used in the analytical model. 7

Table 2. Measured material properties of fiber preform and distribution medium........ 11

INTENTIONALLY LEFT BLANK.

1. Introduction

The vacuum-assisted resin-transfer process (VARTM) process offers numerous cost advantages over traditional resin-transfer molding (RTM) via lower tooling costs, room-temperature processing, and scalability for large structures. Recent advanced technology demonstrators such as the U.S. Navy's Advanced Enclosed Mast Sensor (AEM/S) System, the U.S. Army's Composite Armored Vehicle (CAV), and other Army programs on lightweight composite hull structures for ground vehicles have shown the potential of VARTM technology for the low-cost fabrication of large-scale structures. The VARTM process is also used extensively in commercial applications such as bridge decks, rail cars, and yachts.

The present study focuses on Seemann's Composite Resin Infusion Molding Process (SCRIMP) [1]. In this VARTM-based process, a highly permeable distribution medium is incorporated over a fiber preform as a surface layer. A vacuum is applied on one side of the preform opposite the resin entry gate. During infusion, the resin flows preferentially across the surface and simultaneously through the preform thickness enabling large parts to be fabricated using only vacuum. Resin flow in the VARTM process is three-dimensional (3-D) through anisotropic porous media (i.e., preform). The lay-up of the materials used in the process is shown in Figure 1. In this process, large parts can be infused rapidly using a variety of resins including vinyl esters, phenolics, and epoxies at room temperature under vacuum pressure. Consequently, tooling costs and capital equipment investments are relatively low. VARTM is a closed process offering environmental benefits through reduced emission of volatile organic compounds (VOCs). In very large composite structures, multiple inlet gates are required to ensure complete wet-out of the part prior to gelation of the resin. Selection of distribution media, preforms, and gate/vent locations are typically based on past experience for similar applications. New applications where part thickness, resin properties, or preform characteristics change require costly trial and error process development. Hence, a fundamental understanding of the process physics and associated process models needs to be established and experimentally validated.

Understanding the flow during the impregnation process provides insight into tool design, gate, vent, and sensor placement that can affect part quality. In addition, modeling and simulation of the flow can enable optimization of the process design variables, such as the cycle time and the distance between resin inlets as functions of the permeabilities of the distribution medium and the fiber preform, resin viscosity, and preform thickness. An analytical model [2] has

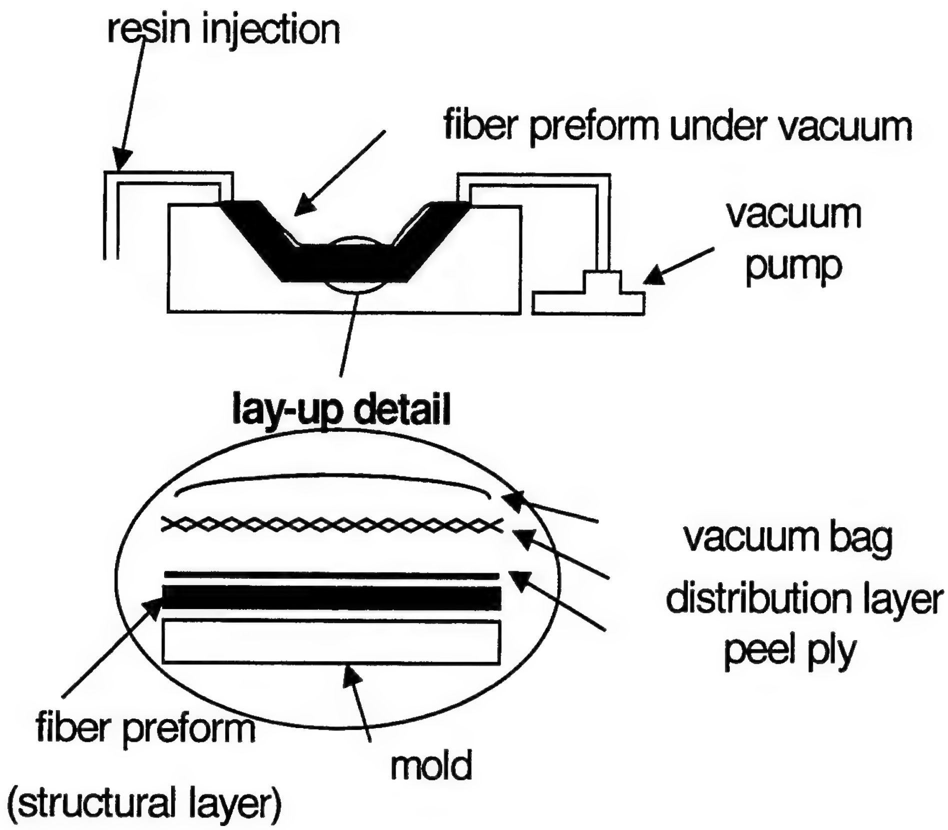

Figure 1. Schematic of the VARTM process.

been developed previously that captures the important process physics. Experimental validation of this model prediction based on independent measurement of input parameters was necessary.

The University of Delaware - Center for Composite Materials (UD-CCM) VARTM test bed is a sophisticated experimental facility for monitoring and controlling the flow of resin in the VARTM process. This test bed integrates SMARTweave [3, 4], a system for 3-D flow and cure monitoring; a digital camera for surface-flow monitoring; an electronic balance for measuring resin-flow rates; a vacuum sensing and control system; automated actuators with sensor feedback for multiple-gate injection; and a LABVIEW-based graphical interface that maintains and controls the process.

In the present study, the test bed was used to experimentally investigate the flow of resin through the thickness of the fiber preform during the VARTM experiments. Experiments were conducted over a wide range of preform thicknesses to assess the accuracy of the analytical model. SMARTweave was used to detect the arrival of the resin at regular intervals through the thickness and along the length of the fiber preform. The lengths and shapes of the flow

front and the arrival times of the resin through the thickness were recorded as a function of preform thickness. The properties of the distribution medium and the fiber preform were measured independently using the test bed in simple one-dimensional (1-D) flow experiments.

In this report, a brief review of VARTM flow modeling, including the analytical model is presented. Details of the VARTM test bed and the experimental procedures are described. Finally, the model predictions are compared with the experimental results and discussed.

2. VARTM Process Modeling

The flow of resin through porous media such as fiber preforms and resin distribution media is governed by Darcy's Law:

$$\mathbf{u} = \frac{-\mathbf{K}}{\mu}.\nabla P. \tag{1}$$

Here **u** is the Darcy's velocity, which is defined as the total flow rate per total cross-sectional area; **K** is the permeability tensor, which characterizes the ease of flow through the fiber perform; and μ is the viscosity of the resin. This, when coupled with the continuity equation for incompressible flow, gives the Laplace equation for the fluid-pressure field inside a region permeated by the fluid.

$$\nabla \cdot (\frac{\mathbf{K}}{\mu}.\nabla P) = 0. \tag{2}$$

The flow simulations can be either two-dimensional (2-D) or 3-D. In 2-D flow modeling [5–7], the flow of resin through the thickness is considered uniform, and the finite element discretization is applied along the other two directions. One such simulation is Liquid Injection Molding Simulation (LIMS), which is based on the finite element/control volume approach [8]. In 2-D simulations, only the permeabilities in the plane of interest are required. In 3-D simulations [9], the pressure and flow in all three directions is solved, and a 3-D permeability tensor is required. Resin Infusion Process Simulation (RIPS) is one such 3-D simulation based on finite element methods without the use of the control volume approach [10]. Usually, the geometry, the material parameters, and the position of resin inlets and outlets are specified before the filling simulation is carried out.

Closed-form analytical solutions have also been derived for the resin flow under simplifying assumptions and for simple geometries and preforms. These

solutions shed light into the role of various process variables, such as vacuum levels, material properties, and preform thickness, and their interactions during processing. Indeed, a closed-form solution of the resin flow during the VARTM process not only enables parametric studies, optimization, and reduction of computational expenses of full-scale simulations, but also offers insight into scalability by identifying appropriate distribution media and resin injection inlet spacings for a required preform material, resin system, and the part dimensions.

3. Review of Analytical Model

In earlier work, a closed-form solution for the flow of resin in VARTM process was derived [2]. The analytical solution for 2-D porous media focuses on a representative cross section (*x-y* plane shown in Figure 2) consisting of the distribution layer (the high permeability material) and the structural layer (the preform material). It is assumed that the flow is well developed and can be divided into two regimes: a saturated region with no through-thickness flow and a flow-front region where the resin is infiltrating into the preform from the distribution medium.

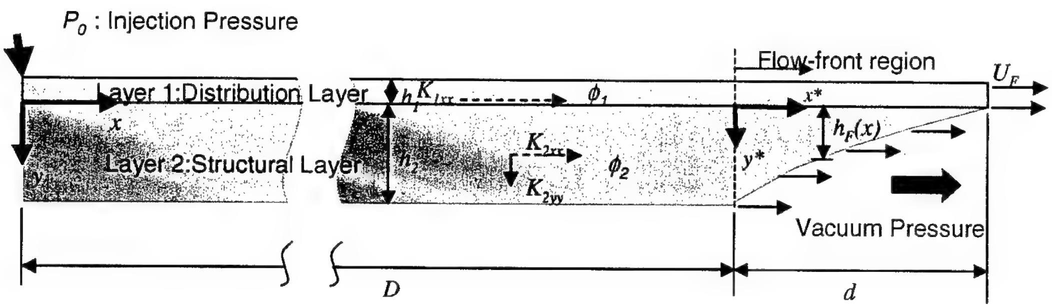

d: region with transverse flow = flow-front length
D: region without transverse flow = length behind the flow-front region
U_F: flow-front velocity
μ: viscosity of resin

Figure 2. Schematic and nomenclature used for the analytical model.

As illustrated in Figure 2, the lay-up of materials is modeled as two distinct layers of permeable materials. The distribution layer (layer 1) is much thinner than the structural layering (layer 2), such that $h_1 << h_2$ where h_1 and h_2 are the respective thicknesses of the two layers. The flow front in the distribution layer is considered uniform (i.e., no gradients in the thickness direction) as the

permeability is isotropic for the distribution layer. The permeability of the distribution layer is K_{1xx} along and across the flow direction, and the permeabilities of the structural layer are K_{2xx} and K_{2yy} in the x and y directions, respectively. The resin viscosity is μ. Vacuum is applied to the preform, and the resin flow is driven by the constant pressure difference, P_0, between the pressure at the inlet, which is atmospheric pressure, and the vacuum pressure at the flow front.

In the saturated region, the flow is 1-D with Darcy's velocities U_1 and U_2 in layer 1 and layer 2, respectively. The length of this saturated region is D, and the pressure at the boundary with the flow region is assumed to be P_D. The second region, illustrated in Figure 3, is the flow-front region where there is transverse flow from the distribution layer to the structural layer. The flow-front region of length d is assumed to maintain its shape, given by $h_F(x)$, and advances with a uniform horizontal velocity of U_F. This is the observed velocity of the resin and not the Darcy's velocity. The transverse velocity of resin infiltration from the distribution layer into the structural layer is u_{12y}. The horizontal velocity in the flow-front region in the distribution layer is denoted by u_{1x} at the distance $x = (D + d) = \Phi_1 U_F$.

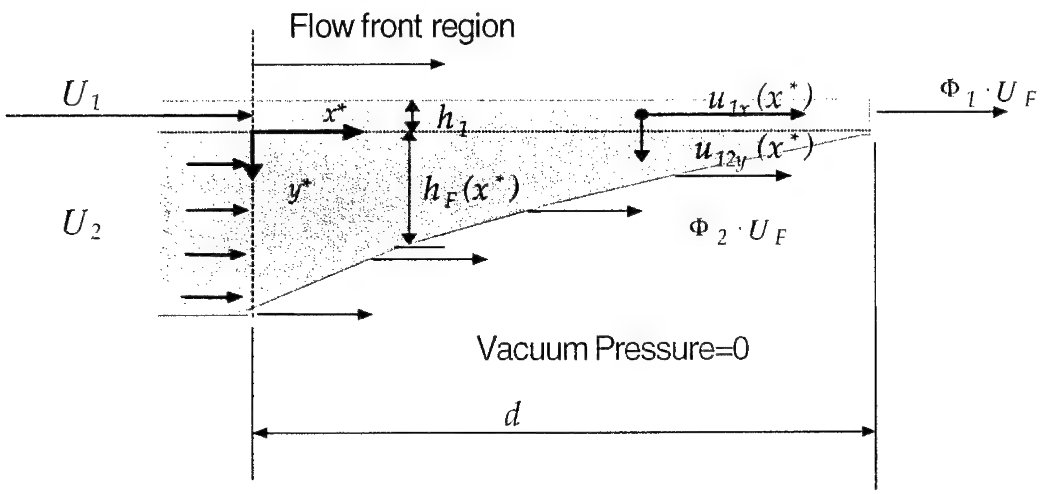

Figure 3. Mass conservation at the flow front.

The flow-front region is assumed to be fully developed and moves with a uniform velocity. The law of conservation of mass and Darcy's law for flow through porous media are applied in each region. The resulting equations are nondimensionalized and are solved to yield the flow-front shape and the development of the saturated region with time. The flow-front shape and the time to fill the length D of the preform are given in equations (3), (4), and (5), respectively:

$$h_F^*(x^*) = \frac{K_{2yy}^*}{6h_1^*} x^{*2} - \sqrt{\frac{2K_{2yy}^*}{3h_1^*} + \frac{\Phi_1 K_{2yy}^*}{\Phi_2 - U_2^*}} x^* + 1, \tag{3}$$

$$t - t_0 = C_1(D^2 - D_0^2) + C_2(D - D_0), \tag{4}$$

$$d^* = \frac{3h_1^*}{\sqrt{K_{2yy}^*}} \left(\sqrt{\frac{\Phi_1}{\Phi_2 - U_2^*} + \frac{2}{3h_1^*}} - \sqrt{\frac{\Phi_1}{\Phi_2 - U_2^*}} \right), \tag{5}$$

where

$$U^* = \frac{U}{U_F}, \quad K^* = \frac{K}{K_{1xx}}, \quad h_F^* = \frac{h_F}{h_2}, \quad x^* = \frac{x - D}{h_2}$$

$$h_1^* = \frac{h_1}{h_2}, \quad d^* = \frac{d}{h_2}, \quad P^* = \frac{P}{P_0}$$

$$U_2^* = \frac{(\Phi_1 h_1^* + \Phi_2)}{(\frac{h}{K_{1xx}^*} + 1)}$$

$$\Gamma = \frac{U_2^*}{K_{2xx}^*}$$

$$\Lambda = \frac{(\Phi_2 - U_2^*)}{K_{2yy}^*} \sqrt{\frac{2K_{2yy}^*}{3h_1^*} + \frac{\Phi_1 K_{2yy}^*}{\Phi_2 - U_2^*}}$$

$$C_1 = \frac{\Gamma \mu}{2K_{1xx} P_0} \text{ and } C_2 = \frac{\mu \Lambda h_2}{K_{1xx} P_0}.$$

The nomenclature used is summarized in Table 1. The variation of the flow-front shape with different numbers of fabric layers in the fiber preform in the structural layer is shown in Figure 4. A parametric study of the length of flow-front region (*d*) demonstrating the effect of the change in permeability of the distribution medium is shown in Figure 5.

Analytical predictions of the length of the saturated region (*D*) with time, the length of the flow-front region (*d*), and the shape of the flow front, $h_F(x)$, are compared to experimental measurements of these parameters as a function of the preform thickness in the next section.

Table 1. Nomenclature used in the analytical model.

$h_F^*(x^*)$	Flow-front shape as a function of distance from the saturated region, x^*
t-t_0	Time to fill saturated length D of the part
D	Length of saturated region
d	Length of flow-front region
U_F	Flow-front velocity
U_2	Flow velocity in saturated region in the preform layer
Φ_1	Porosity of the distribution medium
Φ_2	Porosity of the fiber preform
K_{1xx}	Permeability of distribution layer in the direction of flow
K_{2xx}	Permeability of preform layer in the direction of flow
K_{2yy}	Permeability of preform layer in the direction transverse to the flow
μ	Viscosity of the resin

4. VARTM Test Bed: Description of the Experimental Setup

The VARTM test bed [11, 12] (Figure 6) has been established to allow for sensing and control of the important process parameters. In particular, monitoring of the resin arrival times and flow rates as well as tight control of the applied vacuum levels is needed to study the resin-flow behavior during preform impregnation and to validate process models. The vacuum control system consists of a TESCOM ER3000 pressure controller, a VACCON VDF250 variable-flow vacuum pump (venturi pump), and a VACOON VSSA vacuum sensor for each individual vent. A separate air compressor is needed due to the high flow rates required by

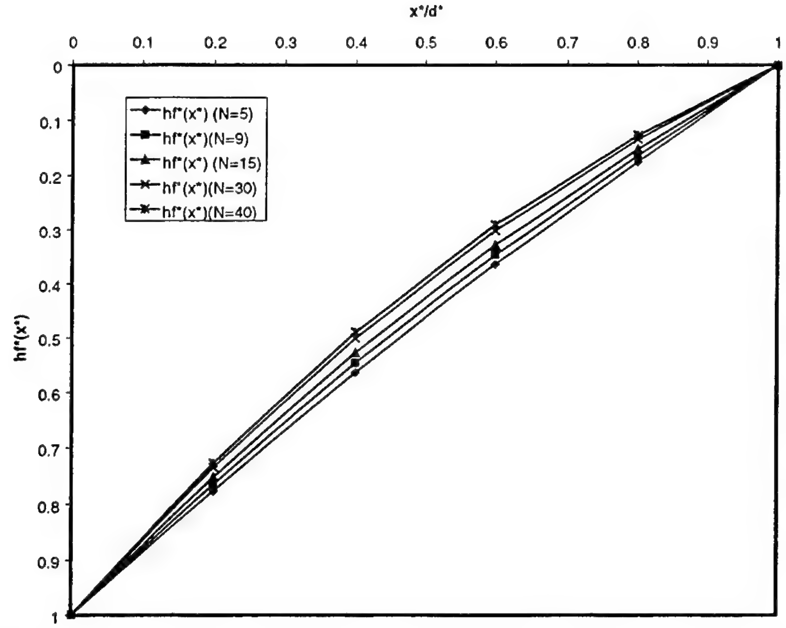

Figure 4. Nominalized flow-front shapes for different number of layers (N) of fiber preforms.

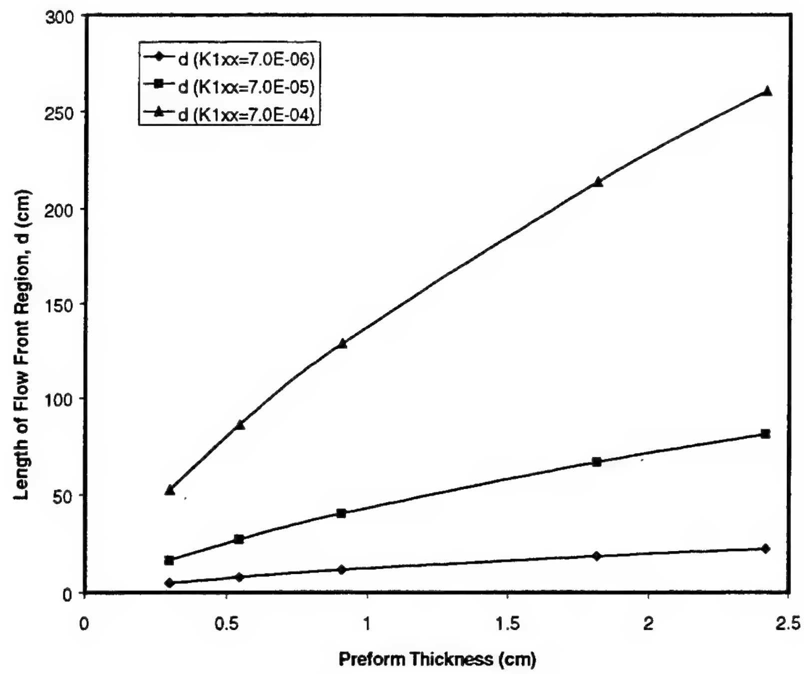

Figure 5. Variation in the length of flow-front region (d) with preform thickness, predicted by the analytical model, for different values of permeability of the distribution medium (a typical permeability value for the distribution medium is 7.05E-05).

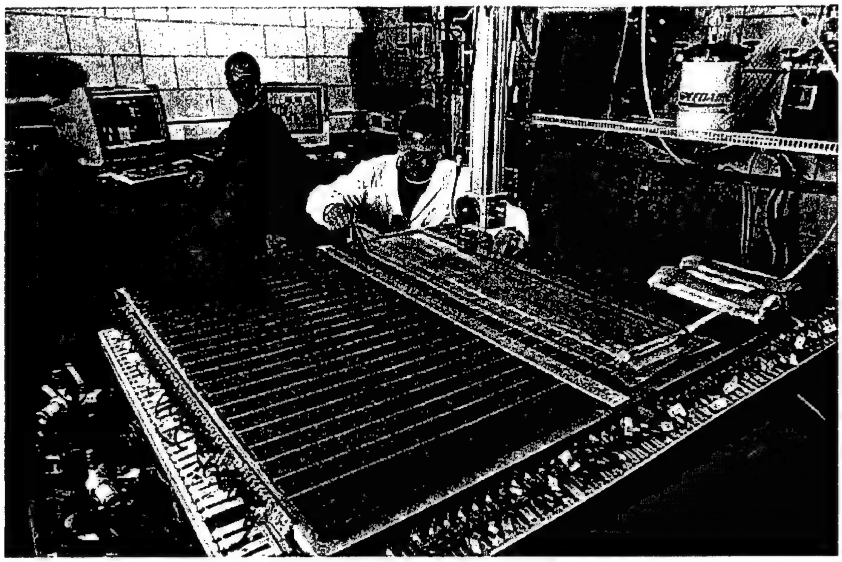

Figure 6. The UD-CCM VARTM workcell that incorporates sensors and enables flow model validation and VARTM automation.

the venturi pumps to maintain the desired inlet pressure at each pressure controller. The pressure controller adjusts the pressure to the venturi pump that generates vacuum. The vacuum level is measured in-situ with the vacuum sensor and is used in a feedback loop to adjust the pressure controller. Together, this system provides accurate and fast control over the vacuum level in the vacuum tank and in the preform near the vent location. A graphical user interface (GUI) written in LABVIEW gives easy access to the control variables and sensor feedback.

Two systems are employed to accurately monitor the resin-flow behavior. A PULNIX TM-1001 charge-coupled device (CCD) camera captures in real time the resin flow on the preform surface. Each individual picture is preprocessed to reduce the pixel noise, and subsequently a threshold algorithm is applied to calculate the wet-out location in the preform. An arrival time map is continuously updated and can be used on-line or off-line to calculate the resin position over time. A second monitoring system is based on the SMARTweave [3, 4] technology. An orthogonal grid of wires (sense and excitation lines) is used to sense the flow-front location. The resistance at each grid point between one excitation and one sense is measured using a voltage-divider system and a data-acquisition board from National Instruments. The junction resistance drops significantly upon resin arrival and indicates the preform wet-out at each location. The current U.S. Army Research Laboratory (ARL)/UD-CCM SMARTweave system enables point sensors to be multiplexed within a 64 × 64 sensor grid. Multiple grids are placed between different layers of the preform to enable 3-D flow monitoring during impregnation.

5. Experimental Procedures

The experimental work consisted of two parts: (1) the measurement of model input properties such as the permeabilities of the preform and distribution media and (2) flow-front measurement with varying preform thickness to validate model predictions. The material properties required by the model include the permeabilities and porosities of the structural layer (i.e., fiber preform [K_{2xx}, K_{2yy}, Φ_2], the distribution medium [K_{1xx}, Φ_1], and the resin [μ]). The resin used in this study was Dow Derakane 411-C50 vinyl ester, while the fiber preform and the distribution layer were made up of 24-oz S2-glass-woven roving fabric and a single layer of shading material from Roxford Fordell, respectively. Permeability-measurement experiments were conducted to measure the permeabilities using the test bed [13]. The porosities were determined using the standard ASTM burn-off test [14].

5.1 3-D Preform Permeabilities

The permeability tensor of the fiber preform has three principal values, k_1, k_2, and k_3. In earlier work, a method to predict all three principal components in one experiment using SMARTweave was developed [13]. This method was used to determine the preform permeability values required for this study. For the material used here (24-oz S2-glass-woven roving fabric), the x, y, and z directions coincide with the principal directions. In the experiment to measure these values, 10–20 layers of the preform were placed under vacuum, without the distribution medium. A number of SMARTweave layers were used at regular spacing between the layers. Bare copper wires were used to minimize the interference on the flow front and a video camera recorded the flow front on the surface of the fiber preform. The data is obtained by the SMARTweave system in this experiment at the nodes of the intersecting grid of wires. The times when the flow front reaches the coordinates of each node (x_i', y_i', z_i', t_i) were recorded. According to the theory, one can relate the arrival times with the preform permeability as detailed by Nedanov et al. [13]:

$$t_{ff,i} = f(k_1, k_2, k_3, k)$$

where

$$k = (k_1 k_2 k_3)^{\frac{1}{3}}. \tag{6}$$

These nonlinear equations are solved to obtain the values of k_1, k_2, and k_3. The central-injection method was used to inject resin into the preform. An inhibitor was used to prevent the premature cure of the resin. The data from the experiment consisted of the flow rate, the video of the flow front on the surface, and the time to reach each SMARTweave node through the thickness.

Additional data include the resin properties (density, viscosity), the size of the injection tube, and the level of vacuum used.

5.2 Permeability of Distribution Medium

The permeability of the distribution medium was measured using an independent 1-D flow experiment. The distribution medium was placed under vacuum and the resin injected into a line-injection source at one end. A video of the flow-front progression with time was used for determining the permeability. The distance traveled by the flow with time was recorded and the permeability determined using the 1-D flow equation:

$$K_{1xx} = \frac{\mu x_f^2}{2 * t * \Delta P}. \tag{7}$$

This experiment was repeated with additional layers of the distribution medium and the corresponding permeability was determined. Three 40-in-long sections with one, two, and three layers of the distribution media were bagged and injected using vinyl ester 411-C50 resin. The 40-in-long panel spans 650 pixels of each image, resulting in a resolution of approximately 0.06 in per pixel. The arrival times of the resin for each image pixel were determined from the video of the flow front. Equation (7) is applied to calculate the permeability of the distribution media. The permeability values are tabulated in Table 2.

Table 2. Measured material properties of fiber preform and distribution medium.

K_{1xx}	7.00E-05 m^2
K_{2xx}	3.63E-07 m^2
K_{2yy}	9.20E-09 m^2
Φ_1	0.9
Φ_2	0.5
μ	85 cP

5.3 Porosities of Fiber Preforms and Distribution Media

Since the volume fractions (and preform porosities, Φ_1 and Φ_2) of the materials change under compaction by vacuum, it was necessary to estimate them using the fabricated panels. The standard ASTM burn-off test [14] was used to determine the volume fractions of the fiber preforms and distribution medium.

5.4 Flow Experiments With Varying Preform Thickness

Flow experiments were conducted to measure the following:

(1) time to fill a particular length of composite (t-t_0),

(2) length of flow front region (d), and

(3) shape of flow front ($h_F^*(x^*)$).

In these experiments, preform thickness was varied by increasing the number of layers of fiber preform (6, 9, 15, 30, and 40 layers). Three-dimensional flow information was generated from the CCD camera that records the flow front at the top surface and the SMARTweave embedded at regular intervals throughout the thickness. In general, flow-front information is measured at a minimum of three locations through the thickness of the fiber preform.

Five different composite panels were manufactured with 6, 9, 15, 30, and 40 layers of 24-oz woven-fabric S2-Glass. One layer of shading material from Roxford Fordell was used as the distribution media. The dimension of each panel was 40 in long and 6 in wide. Twenty-one excitation lines at 2-in spacing were placed on top of the distribution media (parallel to the resin flow front), and 1 sense line was placed at mid-width (perpendicular to the resin flow front) every 3 layers for the 6-, 9-, and 15-layer preforms and 5 layers for the 30- and 40-layer preforms, respectively (Figure 7). This allowed for accurate through-thickness flow measurements at up to 168 sensor locations.

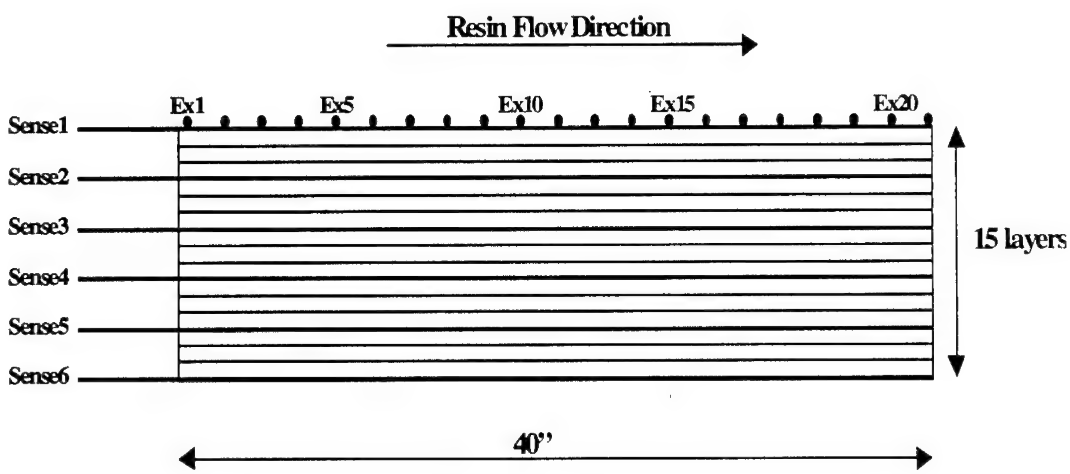

Figure 7. Experimental SMARTweave grid with 21 excitation and 6 sense lines for the 15-layer E-glass preform.

The properties of the materials utilized for the experiments were measured and the results are summarized in Table 2. It is noteworthy that the permeability of a single layer of distribution medium is two to four orders of magnitude higher than that of the preform. The relative magnitudes of the permeabilities clearly indicate that the path of least resistance is initially in the distribution medium.

Furthermore, since $K_{2yy} << K_{2xx} << K_{1xx}$, significant gradients in the flow-front region are developed with increasing preform thickness.

Using the experimental procedure previously outlined, the resin arrival times were recorded throughout the preform. Experimental results are presented in Figures 8–12 for preforms containing 5, 9, 15, 30, and 40 layers, respectively. A number of observations can be made from these results. The first is that the overall fill time increases significantly as the preform thickness increases, ranging from 200 to 1,000 s for the 6- to 40-ply preforms, respectively (the breaks in Figures 11 and 12 are due to the failure of a line of sensors during the injection). The fill time is approximately a linear function of the preform thickness. It was observed that the bottom layer lags behind the resin arrival time at the top surface due to the presence of the high permeability layer, in all cases. The lag time also increases significantly with preform thickness, increasing from 10 s to more than 600 s.

Note that the arrival time for the bottom layer measured experimentally is equivalent to the time taken to fill the saturated region predicted by the model. In Figure 13, model predictions are correlated with experimental measurements over the full range of the preform thickness. The properties of the resin and fiber preform from Table 1 were used for the comparison. The times to fill the bottom layer were compared with those computed using equation (3). Overall, the model accurately predicts the time to fill the preform layer. This also implies that the independent measurements of the permeabilities, the porosities, and the resin viscosity were quite accurate as well. For the thicker preform, some discrepancy is noticed for regions near the inlet where steady state flow may not have been achieved.

Given the location of flow sensors in the preform, arrival times can be used to reconstruct the flow fronts. These results are presented in Figures 14 and 15. Consistent with the description of lag time, the flow front at the bottom lags behind the flow front at the surface. This lag distance ranges from 3/4 in for the 6-ply preform to more than 24 in for the 40-ply preform. This is a significant result because standard industrial practice calls for an inlet spacing of 18 in, which is suitable for thin preforms (where the lag distance is smaller than the inlet spacing), but it should be reassessed for thick preforms, where the lag distance is of the same order of magnitude and often larger than the standard inlet spacing.

The sensor information has been integrated into a complete picture of the resin flow (Figures 14 and 15) and shows that the flow of resin in the VARTM process has an initial transition region near the injection location and a steady flow-front shape thereafter. The variations in the flow-front shape may be caused by local property variations and also due to the discrete nature of the SMARTweave grid. The length of the flow front and hence the lag between resin arrivals at the top and bottom layers shows an increase with the increase in number of layers and, consequently, with the increase in the thickness of the preform.

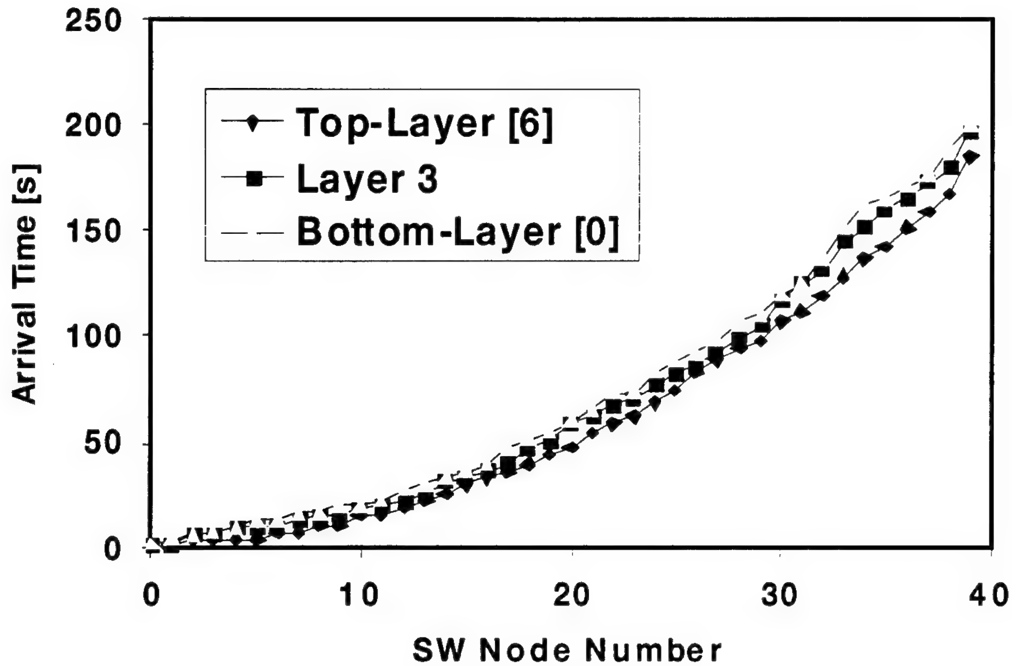

Figure 8. Resin arrival time of 5-layer 411-C50 injection 85cP, 40 in × 6 in.

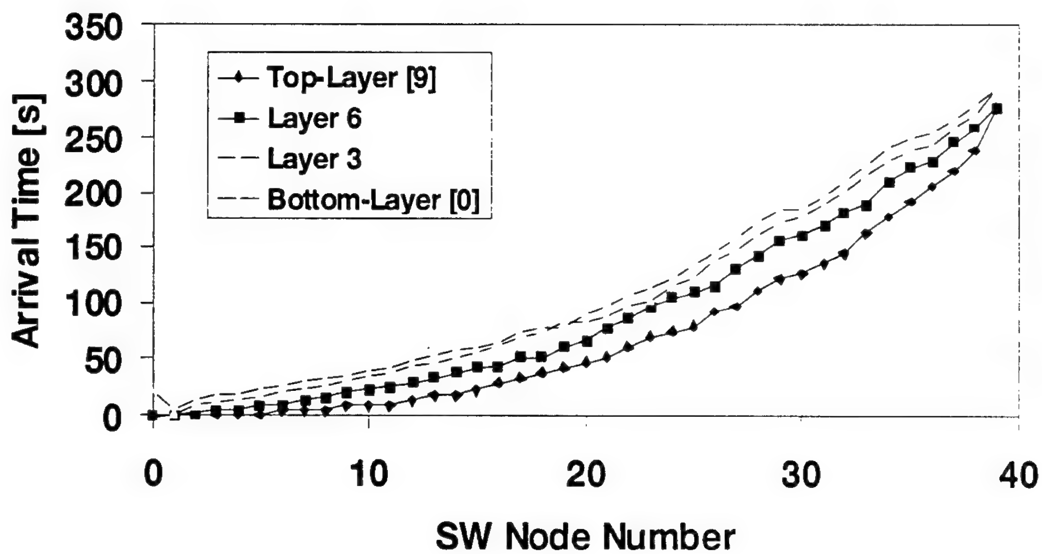

Figure 9. Resin arrival time of 9-layer 411-C50 injection 85cP, 40 in × 6 in.

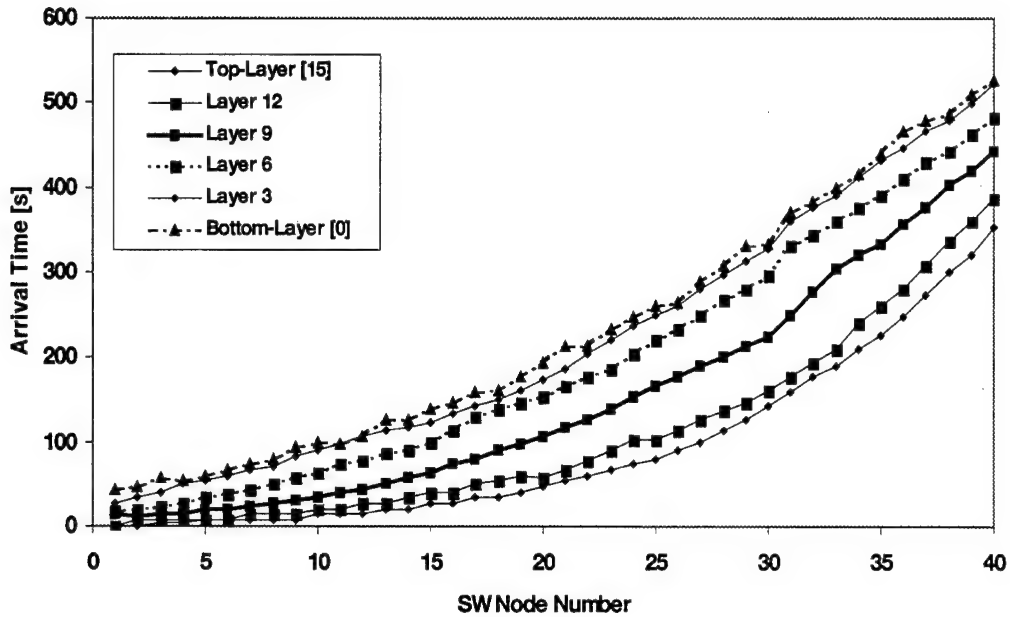

Figure 10. Resin arrival time of 15-layer 411-C50 injection 85cP, 40 in × 6 in.

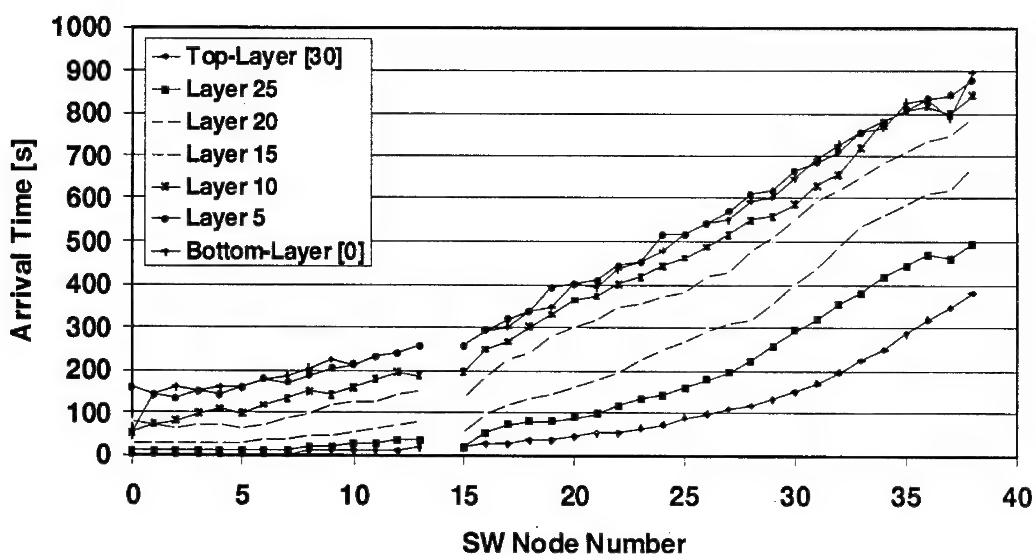

Figure 11. Resin arrival time of 30-layer 411-C50 injection 85cP, 40 in × 6 in.

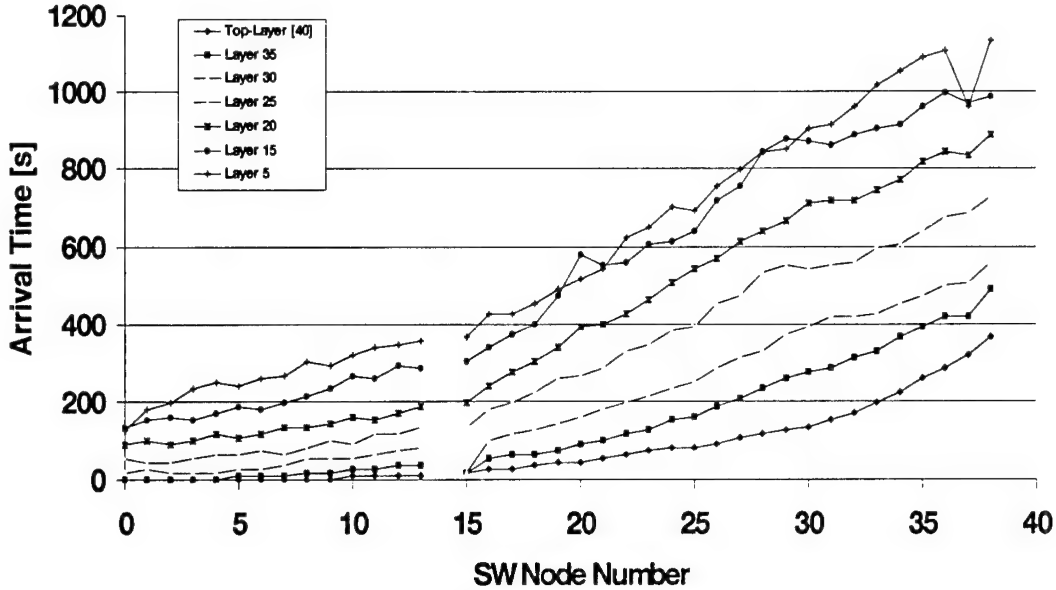

Figure 12. Resin arrival time of 40-layer 411-C50 injection 85cP, 40 in × 6 in.

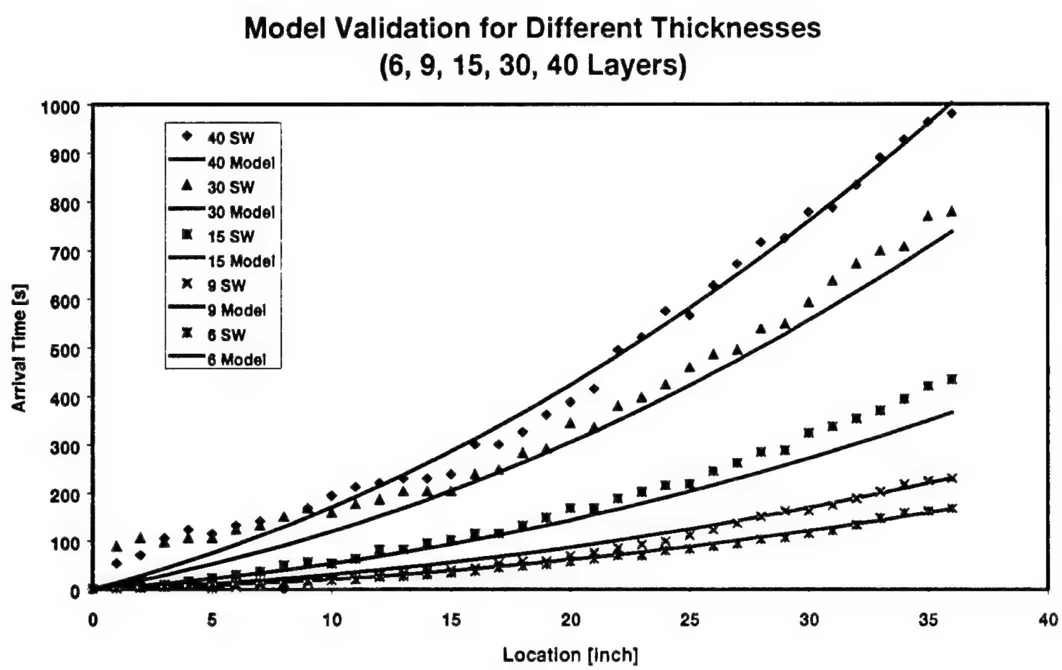

Figure 13. Arrival time of resin at the bottom layer: comparison of model prediction and experimental data from SMARTweave.

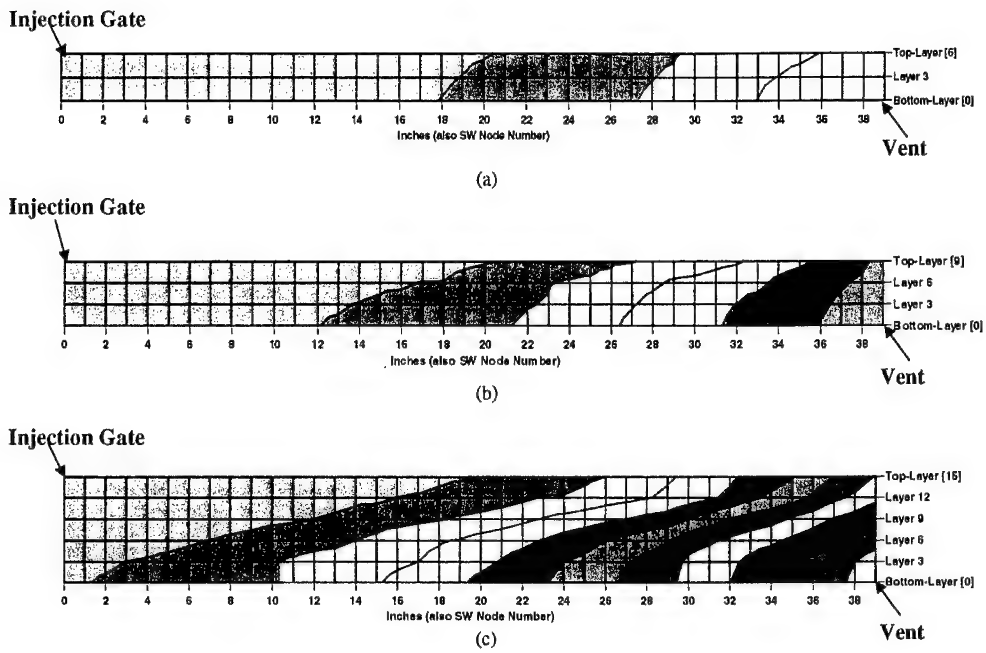

Figure 14. Reconstructed flow fronts from resin arrival data (a) 5 layers of preform material, (b) 9 layers of preform material, and (c) 15 layers of preform material.

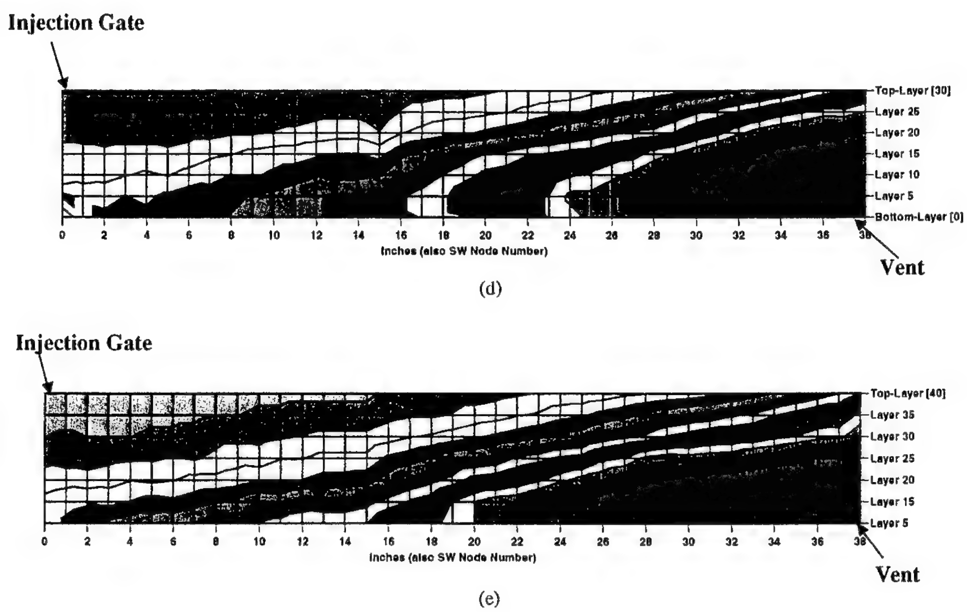

Figure 15. Reconstructed flow fronts from resin arrival data (d) 30 layers of preform and (e) 40 layers of preform.

The lag distance, *'d'*, was measured from the experimental data and was compared to that predicted by the analytical model. The results are presented in Figure 16. The length of the flow front region also shows a good agreement with the model predictions. It can be observed that the length observed from the experiment is always less than that predicted by the model. This is because the model divides the flow into two separate regions—the flow-front region and the saturated region, whereas, there are transition regions at the injection location and between the flow-front and saturated regions, as demonstrated by simulation studies [2]. In effect, the model incorporates the mass flow in these transition regions into the flow-front region, thus over-estimating the length of the flow-front region. The locations of the flow front at any given time were tracked from the experimental data and compared with those predicted by the analytical model. In Figure 17, the locations of the flow-front profile from experiment and those of the model are plotted for each case study used in the experiment. It can be observed that the flow-front locations from the experiments are always less than those predicted by the model for any given x*/d (model). This is due to the overestimation of the length of flow-front region by the analytical model. Also it can be observed that the experimental data is closer to the flow front predicted by the analytical model, as the number of layers of preform increase. This is because, in the development of the model, it was assumed that the thickness of the distribution medium is significantly smaller than that of the structural (fiber preform) layer. As the number of layers of fiber fabric within the preform increases, the accuracy of the analytical model increases and hence the better match between experimental flow front data and the model predictions.

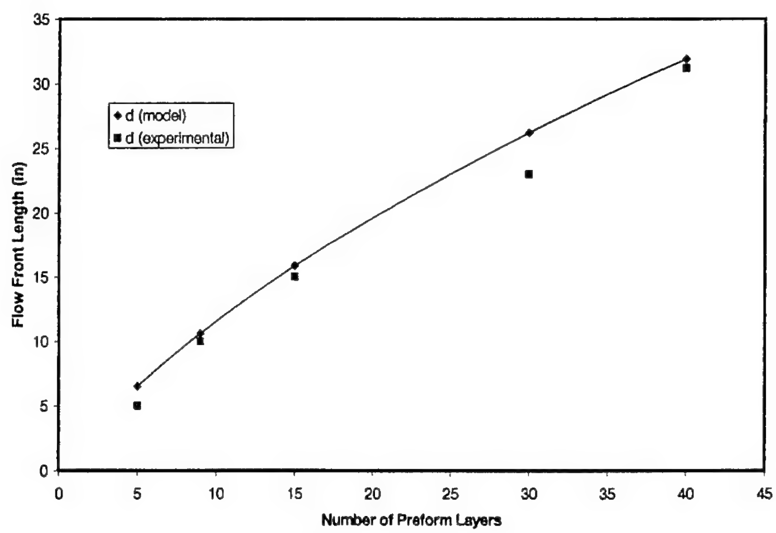

Figure 16. Length of flow region: comparison of model prediction with experimental observations for different number of layers of front-fiber preform.

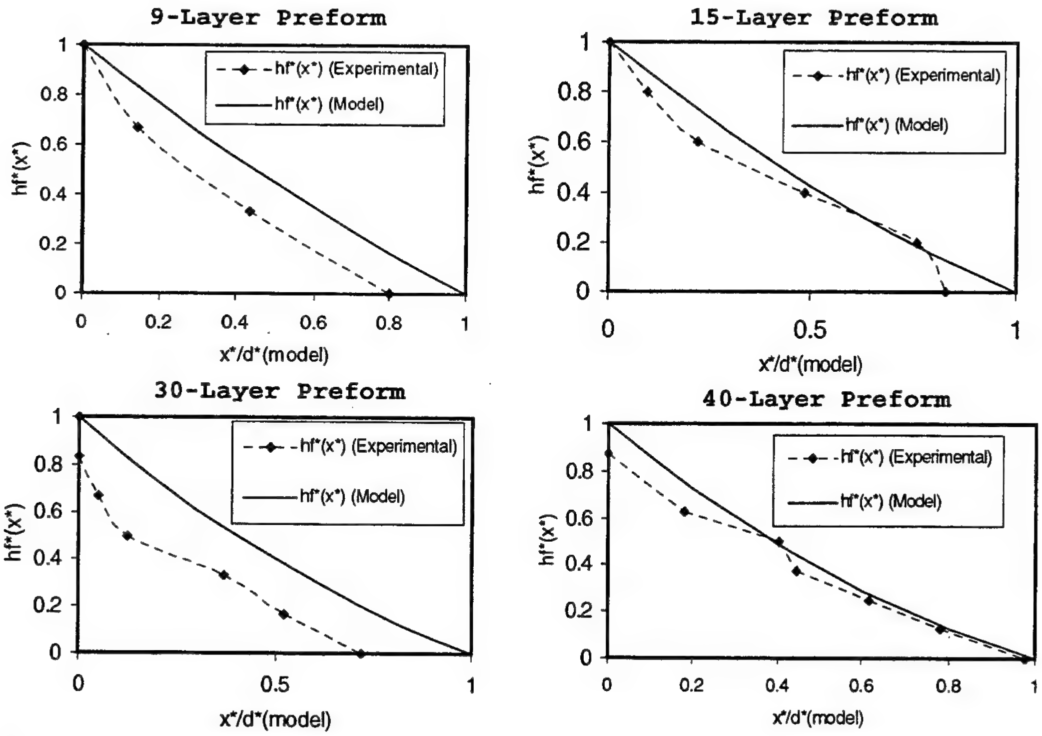

Figure 17. Flow-front profile through the thickness: comparison of model predictions with experimental data for different number of layers of fiber preform.

The experimental data has clearly demonstrated that as the thickness of the structural layer increases, the length of the flow front and the lag time between the top and bottom of mold increases significantly. This has important consequences for the manufacture of large parts by VARTM where a number of injection lines are used in sequence to fill sections of the part. Each line is activated when the resin flow reaches it. Hence, if the resin at the bottom layer lags behind the flow at the top layer, the injection line gets activated prematurely since the section of the fiber preform lying below the injection line is not wetted out. If the lag is large for thick parts, as the experiments demonstrate, there may be formation of "dry spots" or areas that are not fully wetted out because the resin races ahead in the top layer. In order to avoid this problem, the injection lines in the sequential injection of large parts have to be spaced in an optimal manner. Since the bottom layer of the preform cannot be viewed, it is necessary to use a sensor-based control strategy to ensure that each injection line is activated only when the flow front has reached the bottom layer immediately below the line. Hence, these results are also significant because they demonstrate that the closure of inlets based on surface-flow monitoring may result in significant dry-spot formation and thus make a strong case for the need for on-line sensing, control, and optimization of the VARTM process.

6. Conclusions

An experimental study of the resin flow during the VARTM process was undertaken using a VARTM test bed, and the results were compared with an analytical model. The test bed was used to measure the properties of the fiber preform and the flow of resin through the thickness and along the length of the part, using a SMARTweave sensor grid. Experiments were performed using five parts with different numbers of layers of fiber preform. The experiments show that the resin flow in the VARTM process has a steady flow-front shape away from the injection location and that there is a steady lag between the resin flow front at the top and the bottom layers, which increases with the thickness of the preform. The times of arrival at the bottom layer, the length of the flow-front region, and the shape of the flow front were compared to the predictions from the analytical model developed in earlier work and show good agreement. The experiments have yielded a portrait of through-thickness resin flow in VARTM in detail for the first time and demonstrated the need for process optimization and on-line sensing and control, especially in the sequential injection of large parts.

7. References

1. Seemann, III, W. H. "Plastic Transfer Molding Techniques for the Production of Fiber Reinforced Plastic Structures." U. S. Patent 4,902,215, 1990.

2. Hsiao, K. T., R. Mathur, J. W. Gillespie, B. K. Fink, and S. G. Advani. "A Closed Form Solution for the Vacuum Assisted Resin Transfer Molding Process." *ASME Journal of Manufacturing Science and Technology,* vol. 122, no. 2, pp. 291–298, 2000.

3. Walsh, S. M. "In-Situ Sensor Method and Device." U.S. Patent 5,210,499, 1993.

4. Fink, B. K., S. M. Walsh, D. C. DeSchepper, R. L. McCullough, R. C. Don, B. J. Waibel, and J. W. Gillespie, Jr. "Advances in Resin Transfer Molding Flow Monitoring Using SMARTweave Sensors." *Proceedings of the ASME Materials Division,* vol. 69–2, pp. 999–1015, 1995.

5. Bruschke, M. V., and S. G. Advani. "A Numerical Approach to Model Non-isothermal, Viscous Flow With Free Surfaces Through Fibrous Media." *International Journal of Numerical Methods in Fluids,* vol. 19, pp. 575–603, 1991.

6. Trochu, F., R. Gauvin, D. M. Gao, and J.-F. Boudreault. "RTMFLOT - An Integrated Software Environment for the Computer Simulation of the Resin Transfer Molding Process." *Journal of Reinforced Plastics and Composites,* vol. 13, no. 3, 1994.

7. Lee, L. J., W. B. Young, and R. J. Lin. "Mold Filling and Cure Modeling of RTM and SCRIMP Processes." *Composite Structures,* vol. 27, no. 1–2, 1994.

8. Simacek, P., E. M. Sozer, and S. G. Advani. "User Manual for DRAPE 1.1 and LIMS 4.0." Center for Composite Materials, University of Delaware, Newark, DE, 1998.

9. Huang, X., J. W. Gillespie, Jr., T. A. Bogetti, B. K. Fink, D. Heider, and D. A. Eckel, II. "Three-Dimensional and Multi-Domain Cure Simulation of VARTM Composite Structures." Proceedings of the American Society for Composites Thirteenth Technical Conference, Baltimore, MD, 21–23 September 1998.

10. Gallez, X. E., and S. G. Advani. "Numerical Simulations for Impregnation of Fiber Preforms in Composites Manufacturing." Proceedings of the Fourth International Conference on Flow Processes in Composite Materials, University of Wales, 1996.

11. Heider, D., A. Graf, B. K. Fink, and J. W. Gillespie, Jr. "Feedback Control of the Vacuum Assisted Resin Transfer Molding (VARTM) Process." *Proceedings of SPIE - The International Society for Optical Engineering*, vol. 3589, pp. 133–141, 3–4 March 1999.

12. Heider, D., C. Hofmann, and J. W. Gillespie, Jr. "Automation and Control of Large-Scale Composite Parts by VARTM Processing." Proceedings of the 45th International SAMPE Symposium/Exhibition, "Bridging the Centuries With SAMPE's Materials and Processes Technology," Long Beach, CA, 21–25 May 2000.

13. Nedanov, P., S. G. Advani, S. M. Walsh, and B. O. Ballata. "Determination of the Permeability Tensor of Fibrous Reinforcements for VARTM." Proceedings of the ASME, Advances in Aerospace Materials and Structures, AD-Vol. 58, ASME, 1999.

14. American Society for Testing and Materials. *Standard Test Method for Ignition Loss of Cured Reinforced Resin*. ASTM D-2584, West Conshohocken, PA.

NO. OF COPIES	ORGANIZATION
2	DEFENSE TECHNICAL INFORMATION CENTER DTIC OCA 8725 JOHN J KINGMAN RD STE 0944 FT BELVOIR VA 22060-6218
1	HQDA DAMO FDT 400 ARMY PENTAGON WASHINGTON DC 20310-0460
1	OSD OUSD(A&T)/ODDR&E(R) DR R J TREW 3800 DEFENSE PENTAGON WASHINGTON DC 20301-3800
1	COMMANDING GENERAL US ARMY MATERIEL CMD AMCRDA TF 5001 EISENHOWER AVE ALEXANDRIA VA 22333-0001
1	INST FOR ADVNCD TCHNLGY THE UNIV OF TEXAS AT AUSTIN 3925 W BRAKER LN STE 400 AUSTIN TX 78759-5316
1	DARPA SPECIAL PROJECTS OFFICE J CARLINI 3701 N FAIRFAX DR ARLINGTON VA 22203-1714
1	US MILITARY ACADEMY MATH SCI CTR EXCELLENCE MADN MATH MAJ HUBER THAYER HALL WEST POINT NY 10996-1786
1	DIRECTOR US ARMY RESEARCH LAB AMSRL D DR D SMITH 2800 POWDER MILL RD ADELPHI MD 20783-1197

NO. OF COPIES	ORGANIZATION
1	DIRECTOR US ARMY RESEARCH LAB AMSRL CI AI R 2800 POWDER MILL RD ADELPHI MD 20783-1197
3	DIRECTOR US ARMY RESEARCH LAB AMSRL CI LL 2800 POWDER MILL RD ADELPHI MD 20783-1197
3	DIRECTOR US ARMY RESEARCH LAB AMSRL CI IS T 2800 POWDER MILL RD ADELPHI MD 20783-1197
	ABERDEEN PROVING GROUND
2	DIR USARL AMSRL CI LP (BLDG 305)

NO. OF COPIES	ORGANIZATION
1	DIRECTOR US ARMY RESEARCH LAB AMSRL CP CA D SNIDER 2800 POWDER MILL RD ADELPHI MD 20783-1145
1	DIRECTOR US ARMY RESEARCH LAB AMSRL OP SD TA 2800 POWDER MILL RD ADELPHI MD 20783-1145
3	DIRECTOR US ARMY RESEARCH LAB AMSRL OP SD TL 2800 POWDER MILL RD ADELPHI MD 20783-1145
1	DIRECTOR US ARMY RESEARCH LAB AMSRL OP SD TP 2800 POWDER MILL RD ADELPHI MD 20783-1145
1	DIRECTOR DA OASARDA SARD SO 103 ARMY PENTAGON WASHINGTON DC 20310-0103
1	DPTY ASST SECY FOR R&T SARD TT THE PENTAGON RM 3EA79 WASHINGTON DC 20301-7100
1	COMMANDER US ARMY MATERIEL CMD AMXMI INT 5001 EISENHOWER AVE ALEXANDRIA VA 22333-0001
4	COMMANDER US ARMY ARDEC AMSTA AR CC G PAYNE J GEHBAUER C BAULIEU H OPAT PICATINNY ARSENAL NJ 07806-5000

NO. OF COPIES	ORGANIZATION
2	COMMANDER US ARMY ARDEC AMSTA AR AE WW E BAKER J PEARSON PICATINNY ARSENAL NJ 07806-5000
1	COMMANDER US ARMY ARDEC AMSTA AR TD C SPINELLI PICATINNY ARSENAL NJ 07806-5000
1	COMMANDER US ARMY ARDEC AMSTA AR FSE PICATINNY ARSENAL NJ 07806-5000
6	COMMANDER US ARMY ARDEC AMSTA AR CCH A W ANDREWS S MUSALLI R CARR M LUCIANO E LOGSDEN T LOUZEIRO PICATINNY ARSENAL NJ 07806-5000
1	COMMANDER US ARMY ARDEC AMSTA AR CCH P J LUTZ PICATINNY ARSENAL NJ 07806-5000
1	COMMANDER US ARMY ARDEC AMSTA AR FSF T C LIVECCHIA PICATINNY ARSENAL NJ 07806-5000
1	COMMANDER US ARMY ARDEC AMSTA ASF PICATINNY ARSENAL NJ 07806-5000

NO. OF COPIES	ORGANIZATION
1	COMMANDER US ARMY ARDEC AMSTA AR QAC T C C PATEL PICATINNY ARSENAL NJ 07806-5000
1	COMMANDER US ARMY ARDEC AMSTA AR M D DEMELLA PICATINNY ARSENAL NJ 07806-5000
3	COMMANDER US ARMY ARDEC AMSTA AR FSA A WARNASH B MACHAK M CHIEFA PICATINNY ARSENAL NJ 07806-5000
2	COMMANDER US ARMY ARDEC AMSTA AR FSP G M SCHIKSNIS D CARLUCCI PICATINNY ARSENAL NJ 07806-5000
1	COMMANDER US ARMY ARDEC AMSTA AR FSP A P KISATSKY PICATINNY ARSENAL NJ 07806-5000
2	COMMANDER US ARMY ARDEC AMSTA AR CCH C H CHANIN S CHICO PICATINNY ARSENAL NJ 07806-5000
1	COMMANDER US ARMY ARDEC AMSTA AR QAC T D RIGOGLIOSO PICATINNY ARSENAL NJ 07806-5000
1	COMMANDER US ARMY ARDEC AMSTA AR WET T SACHAR BLDG 172 PICATINNY ARSENAL NJ 07806-5000
9	COMMANDER US ARMY ARDEC AMSTA AR CCH B P DONADIA F DONLON P VALENTI C KNUTSON G EUSTICE S PATEL G WAGNECZ R SAYER F CHANG PICATINNY ARSENAL NJ 07806-5000
6	COMMANDER US ARMY ARDEC AMSTA AR CCL F PUZYCKI R MCHUGH D CONWAY E JAROSZEWSKI R SCHLENNER M CLUNE PICATINNY ARSENAL NJ 07806-5000
1	COMMANDER US ARMY ARDEC AMSTA AR SRE D YEE PICATINNY ARSENAL NJ 07806-5000
6	PM SADARM SFAE GCSS SD COL B ELLIS M DEVINE R KOWALSKI W DEMASSI J PRITCHARD S HROWNAK PICATINNY ARSENAL NJ 07806-5000

NO. OF COPIES	ORGANIZATION
1	US ARMY ARDEC INTELLIGENCE SPECIALIST AMSTA AR WEL F M GUERRIERE PICATINNY ARSENAL NJ 07806-5000
2	PEO FIELD ARTILLERY SYS SFAE FAS PM H GOLDMAN T MCWILLIAMS PICATINNY ARSENAL NJ 07806-5000
11	PM TMAS SFAE GSSC TMA R MORRIS C KIMKER D GUZOWICZ E KOPACZ R ROESER R DARCY R MCDANOLDS L D ULISSE C ROLLER J MCGREEN B PATTER PICATINNY ARSENAL NJ 07806-5000
1	COMMANDER US ARMY ARDEC AMSTA AR WEA J BRESCIA PICATINNY ARSENAL NJ 07806-5000
1	COMMANDER US ARMY ARDEC PRODUCTION BASE MODERN ACTY AMSMC PBM K PICATINNY ARSENAL NJ 07806-5000
1	COMMANDER US ARMY TACOM PM ABRAMS SFAE ASM AB 6501 ELEVEN MILE RD WARREN MI 48397-5000

NO. OF COPIES	ORGANIZATION
1	COMMANDER US ARMY TACOM AMSTA SF WARREN MI 48397-5000
3	COMMANDER US ARMY TACOM PM TACTICAL VEHICLES SFAE TVL SFAE TVM SFAE TVH 6501 ELEVEN MILE RD WARREN MI 48397-5000
1	COMMANDER US ARMY TACOM PM BFVS SFAE ASM BV 6501 ELEVEN MILE RD WARREN MI 48397-5000
1	COMMANDER US ARMY TACOM PM AFAS SFAE ASM AF 6501 ELEVEN MILE RD WARREN MI 48397-5000
1	COMMANDER US ARMY TACOM PM RDT&E SFAE GCSS W AB J GODELL 6501 ELEVEN MILE RD WARREN MI 48397-5000
2	COMMANDER US ARMY TACOM PM SURV SYS SFAE ASM SS T DEAN SFAE GCSS W GSI M D COCHRAN 6501 ELEVEN MILE RD WARREN MI 48397-5000
1	US ARMY CERL R LAMPO 2902 NEWMARK DR CHAMPAIGN IL 61822

NO. OF COPIES	ORGANIZATION
1	COMMANDER US ARMY TACOM PM SURVIVABLE SYSTEMS SFAE GCSS W GSI H M RYZYI 6501 ELEVEN MILE RD WARREN MI 48397-5000
1	COMMANDER US ARMY TACOM PM BFV SFAE GCSS W BV S DAVIS 6501 ELEVEN MILE RD WARREN MI 48397-5000
1	COMMANDER US ARMY TACOM PM LIGHT TACTICAL VHCLS AMSTA TR S A J MILLS MS 209 6501 ELEVEN MILE RD WARREN MI 48397-5000
1	COMMANDER US ARMY TACOM CHIEF ABRAMS TESTING SFAE GCSS W AB QT T KRASKIEWICZ 6501 ELEVEN MILE RD WARREN MI 48397-5000
1	COMMANDER WATERVLIET ARSENAL SMCWV QAE Q B VANINA BLDG 44 WATERVLIET NY 12189-4050
1	COMMANDER WATERVLIET ARSENAL SMCWV SPM T MCCLOSKEY BLDG 253 WATERVLIET NY 12189-4050
2	TSM ABRAMS ATZK TS S JABURG W MEINSHAUSEN FT KNOX KY 40121

NO. OF COPIES	ORGANIZATION
15	COMMANDER US ARMY TACOM AMSTA TR R J CHAPIN R MCCLELLAND D THOMAS J BENNETT D HANSEN AMSTA JSK S GOODMAN J FLORENCE K IYER D TEMPLETON A SCHUMACHER AMSTA TR D D OSTBERG L HINOJOSA B RAJU AMSTA CS SF H HUTCHINSON F SCHWARZ WARREN MI 48397-5000
3	ARMOR SCHOOL ATZK TD R BAUEN J BERG A POMEY FT KNOX KY 40121
11	BENET LABORATORIES AMSTA AR CCB R FISCELLA G D ANDREA E KATHE M SCAVULO G SPENCER P WHEELER K MINER J VASILAKIS G FRIAR R HASENBEIN AMSTA CCB R S SOPOK WATERVLIET NY 12189-4050
2	HQ IOC TANK AMMUNITION TEAM AMSIO SMT R CRAWFORD W HARRIS ROCK ISLAND IL 61299-6000

NO. OF COPIES	ORGANIZATION
2	DAVID TAYLOR RESEARCH CTR R ROCKWELL W PHYILLAIER BETHESDA MD 20054-5000
2	COMMANDER US ARMY AMCOM AVIATION APPLIED TECH DIR J SCHUCK FT EUSTIS VA 23604-5577
1	DIRECTOR US ARMY AMCOM SFAE AV RAM TV D CALDWELL BLDG 5300 REDSTONE ARSENAL AL 35898
2	US ARMY CORPS OF ENGINEERS CERD C T LIU CEW ET T TAN 20 MASS AVE NW WASHINGTON DC 20314
1	US ARMY COLD REGIONS RSCH & ENGRNG LAB P DUTTA 72 LYME RD HANOVER NH 03755
1	SYSTEM MANAGER ABRAMS ATZK TS LTC J H NUNN BLDG 1002 RM 110 FT KNOX KY 40121
1	USA SBCCOM PM SOLDIER SPT AMSSB PM RSS A J CONNORS KANSAS ST NATICK MA 01760-5057
3	BALLISTICS TEAM AMSSB RIP PHIL CUNNIFF JOHN SONG WALTER ZUKAS KANSAS ST NATICK MA 01760-5057
2	MATERIAL SCIENCE TEAM AMSSB RSS JEAN HERBERT MICHAEL SENNETT KANSAS ST NATICK MA 01760-5057
2	OFC OF NAVAL RESEARCH D SIEGEL CODE 351 J KELLY 800 N QUINCY ST ARLINGTON VA 22217-5660
1	NAVAL SURFACE WARFARE CTR DAHLGREN DIV CODE G06 DAHLGREN VA 22448
1	NAVAL SURFACE WARFARE CTR TECH LIBRARY CODE 323 17320 DAHLGREN RD DAHLGREN VA 22448
1	NAVAL SURFACE WARFARE CTR CRANE DIVISION M JOHNSON CODE 20H4 LOUISVILLE KY 40214-5245
8	DIRECTOR US ARMY NATIONAL GROUND INTELLIGENCE CTR D LEITER M HOLTUS M WOLFE S MINGLEDORF J GASTON W GSTATTENBAUER R WARNER J CRIDER 220 SEVENTH ST NE CHARLOTTESVILLE VA 22091
3	NAVAL RESEARCH LAB I WOLOCK CODE 6383 R BADALIANCE CODE 6304 L GAUSE WASHINGTON DC 20375
2	NAVAL SURFACE WARFARE CTR U SORATHIA C WILLIAMS CD 6551 9500 MACARTHUR BLVD WEST BETHESDA MD 20817

NO. OF COPIES	ORGANIZATION
6	US ARMY SBCCOM SOLDIER SYSTEMS CENTER BALLISTICS TEAM J WARD MARINE CORPS TEAM J MACKIEWICZ BUS AREA ADVOCACY TEAM W HASKELL AMSSB RCP SS W NYKVIST T MERRILL S BEAUDOIN KANSAS ST NATICK MA 01760-5019
9	US ARMY RESEARCH OFC A CROWSON J CHANDRA H EVERETT J PRATER R SINGLETON G ANDERSON D STEPP D KISEROW J CHANG PO BOX 12211 RESEARCH TRIANGLE PARK NC 27709-2211
8	NAVAL SURFACE WARFARE CTR J FRANCIS CODE G30 D WILSON CODE G32 R D COOPER CODE G32 J FRAYSSE CODE G33 E ROWE CODE G33 T DURAN CODE G33 L DE SIMONE CODE G33 R HUBBARD CODE G33 DAHLGREN VA 22448
2	COMMANDER NAVAL SURFACE WARFARE CTR CARDEROCK DIVISION R PETERSON CODE 2020 M CRITCHFIELD CODE 1730 BETHESDA MD 20084
1	NAVAL SEA SYSTEMS CMD D LIESE 2531 JEFFERSON DAVIS HWY ARLINGTON VA 22242-5160

NO. OF COPIES	ORGANIZATION
1	NAVAL SURFACE WARFARE CTR M LACY CODE B02 17320 DAHLGREN RD DAHLGREN VA 22448
2	NAVAL SURFACE WARFARE CTR CARDEROCK DIVISION R CRANE CODE 2802 C WILLIAMS CODE 6553 3A LEGGETT CIR BETHESDA MD 20054-5000
1	EXPEDITIONARY WARFARE DIV N85 F SHOUP 2000 NAVY PENTAGON WASHINGTON DC 20350-2000
1	AFRL MLBC 2941 P ST RM 136 WRIGHT PATTERSON AFB OH 45433-7750
1	AFRL MLSS R THOMSON 2179 12TH ST RM 122 WRIGHT PATTERSON AFB OH 45433-7718
2	AFRL F ABRAMS J BROWN BLDG 653 2977 P ST STE 6 WRIGHT PATTERSON AFB OH 45433-7739
1	WATERWAYS EXPERIMENT D SCOTT 3909 HALLS FERRY RD SC C VICKSBURG MS 39180
5	DIRECTOR LLNL R CHRISTENSEN S DETERESA F MAGNESS M FINGER MS 313 M MURPHY L 282 PO BOX 808 LIVERMORE CA 94550

NO. OF COPIES	ORGANIZATION
1	AFRL MLS OL L COULTER 7278 4TH ST BLDG 100 BAY D HILL AFB UT 84056-5205
1	OSD JOINT CCD TEST FORCE OSD JCCD R WILLIAMS 3909 HALLS FERRY RD VICKSBURG MS 29180-6199
1	DEFENSE NUCLEAR AGENCY INNOVATIVE CONCEPTS DIV 6801 TELEGRAPH RD ALEXANDRIA VA 22310-3398
3	DARPA M VANFOSSEN S WAX L CHRISTODOULOU 3701 N FAIRFAX DR ARLINGTON VA 22203-1714
2	FAA TECH CENTER P SHYPRYKEVICH AAR 431 ATLANTIC CITY NJ 08405
2	SERDP PROGRAM OFC PM P2 C PELLERIN B SMITH 901 N STUART ST STE 303 ARLINGTON VA 22203
1	FAA MIL HDBK 17 CHAIR L ILCEWICZ 1601 LIND AVE SW ANM 115N RESTON VA 98055
1	US DEPT OF ENERGY OFC OF ENVIRONMENTAL MANAGEMENT P RITZCOVAN 19901 GERMANTOWN RD GERMANTOWN MD 20874-1928

NO. OF COPIES	ORGANIZATION
1	DIRECTOR LLNL F ADDESSIO MS B216 PO BOX 1633 LOS ALAMOS NM 87545
1	OAK RIDGE NATIONAL LABORATORY R M DAVIS PO BOX 2008 OAK RIDGE TN 37831-6195
3	DIRECTOR SANDIA NATIONAL LABS APPLIED MECHANICS DEPT MS 9042 J HANDROCK Y R KAN J LAUFFER PO BOX 969 LIVERMORE CA 94551-0969
1	OAK RIDGE NATIONAL LABORATORY C EBERLE MS 8048 PO BOX 2008 OAK RIDGE TN 37831
1	OAK RIDGE NATIONAL LABORATORY C D WARREN MS 8039 PO BOX 2008 OAK RIDGE TN 37831
7	NIST R PARNAS J DUNKERS M VANLANDINGHAM MS 8621 J CHIN MS 8621 D HUNSTON MS 8543 J MARTIN MS 8621 D DUTHINH MS 8611 100 BUREAU DR GAITHERSBURG MD 20899
1	HYDROGEOLOGIC INC SERDP ESTCP SPT OFC S WALSH 1155 HERNDON PKWY STE 900 HERNDON VA 20170

NO. OF COPIES	ORGANIZATION
3	NASA LANGLEY RSCH CTR AMSRL VS W ELBER MS 266 F BARTLETT JR MS 266 G FARLEY MS 266 HAMPTON VA 23681-0001
1	NASA LANGLEY RSCH CTR T GATES MS 188E HAMPTON VA 23661-3400
1	FHWA E MUNLEY 6300 GEORGETOWN PIKE MCLEAN VA 22101
4	CYTEC FIBERITE R DUNNE D KOHLI M GILLIO R MAYHEW 1300 REVOLUTION ST HAVRE DE GRACE MD 21078
1	USDOT FEDERAL RAILRD M FATEH RDV 31 WASHINGTON DC 20590
1	CENTRAL INTLLGNC AGNCY OTI WDAG GT W L WALTMAN PO BOX 1925 WASHINGTON DC 20505
1	MARINE CORPS INTLLGNC ACTVTY D KOSITZKE 3300 RUSSELL RD STE 250 QUANTICO VA 22134-5011
1	DIRECTOR NATIONAL GRND INTLLGNC CTR IANG TMT 220 SEVENTH ST NE CHARLOTTESVILLE VA 22902-5396
1	SIOUX MFG B KRIEL PO BOX 400 FT TOTTEN ND 58335

NO. OF COPIES	ORGANIZATION
1	DIRECTOR DEFENSE INTLLGNC AGNCY TA 5 K CRELLING WASHINGTON DC 20310
1	ADVANCED GLASS FIBER YARNS T COLLINS 281 SPRING RUN LANE STE A DOWNINGTON PA 19335
1	COMPOSITE MATERIALS INC D SHORTT 19105 63 AVE NE PO BOX 25 ARLINGTON WA 98223
1	JPS GLASS L CARTER PO BOX 260 SLATER RD SLATER SC 29683
1	COMPOSITE MATERIALS INC R HOLLAND 11 JEWEL CT ORINDA CA 94563
1	COMPOSITE MATERIALS INC C RILEY 14530 S ANSON AVE SANTA FE SPRINGS CA 90670
2	COMPOSIX D BLAKE L DIXON 120 O NEILL DR HEBRUN OH 43025
2	SIMULA J COLTMAN R HUYETT 10016 S 51ST ST PHOENIX AZ 85044
2	PROTECTION MATERIALS INC M MILLER F CRILLEY 14000 NW 58 CT MIAMI LAKES FL 33014

NO. OF COPIES	ORGANIZATION
3	FOSTER MILLER J J GASSNER M ROYLANCE W ZUKAS 195 BEAR HILL RD WALTHAM MA 02354-1196
1	ROM DEVELOPMENT CORP R O MEARA 136 SWINEBURNE ROW BRICK MARKET PLACE NEWPORT RI 02840
2	TEXTRON SYSTEMS T FOLTZ M TREASURE 201 LOWELL ST WILMINGTON MA 08870-2941
1	GLCC INC J RAY 103 TRADE ZONE DR STE 26C WEST COLUMBIA SC 29170
1	O GARA HESS & EISENHARDT M GILLESPIE 9113 LESAINT DR FAIRFIELD OH 45014
2	MILLIKEN RSCH CORP H KUHN M MACLEOD PO BOX 1926 SPARTANBURG SC 29303
1	CONNEAUGHT INDUSTRIES INC J SANTOS PO BOX 1425 COVENTRY RI 02816
2	BATTELLE NATICK OPNS J CONNORS B HALPIN 209 W CENTRAL ST STE 302 NATICK MA 01760
1	ARMTEC DEFENSE PRODUCTS S DYER 85 901 AVE 53 PO BOX 848 COACHELLA CA 92236

NO. OF COPIES	ORGANIZATION
3	PACIFIC NORTHWEST LAB M SMITH G VAN ARSDALE R SHIPPELL PO BOX 999 RICHLAND WA 99352
8	ALLIANT TECHSYSTEMS INC C CANDLAND MN11 2830 C AAKHUS MN11 2830 B SEE MN11 2439 N VLAHAKUS MN11 2145 R DOHRN MN11 2830 S HAGLUND MN11 2439 M HISSONG MN11 2830 D KAMDAR MN11 2830 600 SECOND ST NE HOPKINS MN 55343-8367
2	AMOCO PERFORMANCE PRODUCTS M MICHNO JR J BANISAUKAS 4500 MCGINNIS FERRY RD ALPHARETTA GA 30202-3944
1	SAIC M PALMER 1410 SPRING HILL RD STE 400 MS SH4 5 MCLEAN VA 22102
1	SAIC G CHRYSSOMALLIS 3800 W 80TH ST STE 1090 BLOOMINGTON MN 55431
1	AAI CORPORATION T G STASTNY PO BOX 126 HUNT VALLEY MD 21030-0126
1	APPLIED COMPOSITES W GRISCH 333 NORTH SIXTH ST ST CHARLES IL 60174
1	CUSTOM ANALYTICAL ENG SYS INC A ALEXANDER 13000 TENSOR LANE NE FLINTSTONE MD 21530

NO. OF COPIES	ORGANIZATION
3	ALLIANT TECHSYSTEMS INC J CONDON E LYNAM J GERHARD WV01 16 STATE RT 956 PO BOX 210 ROCKET CENTER WV 26726-0210
1	OFC DEPUTY UNDER SEC DEFNS JAMES THOMPSON 1745 JEFFERSON DAVIS HWY CRYSTAL SQ 4 STE 501 ARLINGTON VA 22202
1	PROJECTILE TECHNOLOGY INC 515 GILES ST HAVRE DE GRACE MD 21078
5	AEROJET GEN CORP D PILLASCH T COULTER C FLYNN D RUBAREZUL M GREINER 1100 WEST HOLLYVALE ST AZUSA CA 91702-0296
3	HEXCEL INC R BOE PO BOX 18748 SALT LAKE CITY UT 84118
1	HERCULES INC HERCULES PLAZA WILMINGTON DE 19894
1	BRIGS COMPANY J BACKOFEN 2668 PETERBOROUGH ST HERNDON VA 22071-2443
1	ZERNOW TECHNICAL SERVICES L ZERNOW 425 W BONITA AVE STE 208 SAN DIMAS CA 91773
1	OLIN CORPORATION L WHITMORE 10101 NINTH ST NORTH ST PETERSBURG FL 33702

NO. OF COPIES	ORGANIZATION
2	OLIN CORPORATION FLINCHBAUGH DIV E STEINER B STEWART PO BOX 127 RED LION PA 17356
1	GKN AEROSPACE D OLDS 15 STERLING DR WALLINGFORD CT 06492
5	SIKORSKY AIRCRAFT G JACARUSO T CARSTENSAN B KAY S GARBO MS S330A J ADELMANN 6900 MAIN ST PO BOX 9729 STRATFORD CT 06497-9729
1	PRATT & WHITNEY C WATSON 400 MAIN ST MS 114 37 EAST HARTFORD CT 06108
1	AEROSPACE CORP G HAWKINS M4 945 2350 E EL SEGUNDO BLVD EL SEGUNDO CA 90245
2	CYTEC FIBERITE M LIN W WEB 1440 N KRAEMER BLVD ANAHEIM CA 92806
1	HEXCEL T BITZER 11711 DUBLIN BLVD DUBLIN CA 94568
1	BOEING R BOHLMANN PO BOX 516 MC 5021322 ST LOUIS MO 63166-0516
1	UDLP G THOMAS PO BOX 58123 SANTA CLARA CA 95052

NO. OF COPIES	ORGANIZATION
2	UDLP R BARRETT MAIL DROP M53 V HORVATICH MAIL DROP M53 328 W BROKAW RD SANTA CLARA CA 95052-0359
3	UDLP GROUND SYSTEMS DIVISION M PEDRAZZI MAIL DROP N09 A LEE MAIL DROP N11 M MACLEAN MAIL DROP N06 1205 COLEMAN AVE SANTA CLARA CA 95052
4	UDLP R BRYNSVOLD P JANKE MS 170 4800 EAST RIVER RD MINNEAPOLIS MN 55421-1498
1	UDLP D MARTIN PO BOX 359 SANTA CLARA CA 95052
2	BOEING DFNSE & SPACE GP W HAMMOND S 4X55 J RUSSELL S 4X55 PO BOX 3707 SEATTLE WA 98124-2207
2	BOEING ROTORCRAFT P MINGURT P HANDEL 800 B PUTNAM BLVD WALLINGFORD PA 19086
1	BOEING DOUGLAS PRODUCTS DIV L J HART SMITH 3855 LAKEWOOD BLVD D800 0019 LONG BEACH CA 90846-0001
1	LOCKHEED MARTIN S REEVE 8650 COBB DR D 73 62 MZ 0648 MARIETTA GA 30063-0648

NO. OF COPIES	ORGANIZATION
1	LOCKHEED MARTIN SKUNK WORKS D FORTNEY 1011 LOCKHEED WAY PALMDALE CA 93599-2502
1	LOCKHEED MARTIN R FIELDS 1195 IRWIN CT WINTER SPRINGS FL 32708
1	MATERIALS SCIENCES CORP B W ROSEN 500 OFC CENTER DR STE 250 FT WASHINGTON PA 19034
1	NORTHRUP GRUMMAN CORP ELECTRONIC SENSORS & SYSTEMS DIV E SCHOCH MS V 16 1745A W NURSERY RD LINTHICUM MD 21090
2	NORTHROP GRUMMAN ENVIRONMENTAL PROGRAMS R OSTERMAN A YEN 8900 E WASHINGTON BLVD PICO RIVERA CA 90660
1	GDLS DIVISION D BARTLE PO BOX 1901 WARREN MI 48090
2	GDLS D REES M PASIK PO BOX 2074 WARREN MI 48090-2074
1	GDLS MUSKEGON OPERATIONS W SOMMERS JR 76 GETTY ST MUSKEGON MI 49442

NO. OF COPIES	ORGANIZATION
1	GENERAL DYNAMICS AMPHIBIOUS SYS SURVIVABILITY LEAD G WALKER 991 ANNAPOLIS WAY WOODBRIDGE VA 22191
6	INST FOR ADVANCED TECH H FAIR I MCNAB P SULLIVAN S BLESS W REINECKE C PERSAD 3925 W BRAKER LN STE 400 AUSTIN TX 78759-5316
2	CIVIL ENGR RSCH FOUNDATION PRESIDENT H BERNSTEIN R BELLE 1015 15TH ST NW STE 600 WASHINGTON DC 20005
1	ARROW TECH ASSO 1233 SHELBURNE RD STE D8 SOUTH BURLINGTON VT 05403-7700
1	R EICHELBERGER CONSULTANT 409 W CATHERINE ST BEL AIR MD 21014-3613
1	UCLA MANE DEPT ENGR IV H T HAHN LOS ANGELES CA 90024-1597
2	UNIV OF DAYTON RESEARCH INST R Y KIM A K ROY 300 COLLEGE PARK AVE DAYTON OH 45469-0168
1	MIT P LAGACE 77 MASS AVE CAMBRIDGE MA 01887

NO. OF COPIES	ORGANIZATION
1	IIT RESEARCH CENTER D ROSE 201 MILL ST ROME NY 13440-6916
1	GA TECH RSCH INST GA INST OF TCHNLGY P FRIEDERICH ATLANTA GA 30392
1	MICHIGAN ST UNIV MSM DEPT R AVERILL 3515 EB EAST LANSING MI 48824-1226
1	UNIV OF KENTUCKY L PENN 763 ANDERSON HALL LEXINGTON KY 40506-0046
1	UNIV OF WYOMING D ADAMS PO BOX 3295 LARAMIE WY 82071
2	PENN STATE UNIV R MCNITT C BAKIS 212 EARTH ENGR SCIENCES BLDG UNIVERSITY PARK PA 16802
1	PENN STATE UNIV R S ENGEL 245 HAMMOND BLDG UNIVERSITY PARK PA 16801
1	PURDUE UNIV SCHOOL OF AERO & ASTRO C T SUN W LAFAYETTE IN 47907-1282
1	STANFORD UNIV DEPT OF AERONAUTICS & AEROBALLISTICS S TSAI DURANT BLDG STANFORD CA 94305

NO. OF COPIES	ORGANIZATION
1	UNIV OF DAYTON J M WHITNEY COLLEGE PARK AVE DAYTON OH 45469-0240
7	UNIV OF DELAWARE CTR FOR COMPOSITE MTRLS J GILLESPIE M SANTARE G PALMESE S YARLAGADDA S ADVANI D HEIDER D KUKICH 201 SPENCER LABORATORY NEWARK DE 19716
1	DEPT OF MATERIALS SCIENCE & ENGINEERING UNIVERSITY OF ILLINOIS AT URBANA CHAMPAIGN J ECONOMY 1304 WEST GREEN ST 115B URBANA IL 61801
1	NORTH CAROLINA STATE UNIV CIVIL ENGINEERING DEPT W RASDORF PO BOX 7908 RALEIGH NC 27696-7908
1	UNIV OF MARYLAND DEPT OF AEROSPACE ENGNRNG A J VIZZINI COLLEGE PARK MD 20742
3	UNIV OF TEXAS AT AUSTIN CTR FOR ELECTROMECHANICS J PRICE A WALLS J KITZMILLER 10100 BURNET RD AUSTIN TX 78758-4497
3	VA POLYTECHNICAL INST & STATE UNIV DEPT OF ESM M W HYER K REIFSNIDER R JONES BLACKSBURG VA 24061-0219

NO. OF COPIES	ORGANIZATION
1	DREXEL UNIV A S D WANG 32ND & CHESTNUT ST PHILADELPHIA PA 19104
1	SOUTHWEST RSCH INST ENGR & MATL SCIENCES DIV J RIEGEL 6220 CULEBRA RD PO DRAWER 28510 SAN ANTONIO TX 78228-0510
	ABERDEEN PROVING GROUND
1	US ARMY MATERIEL SYSTEMS ANALYSIS ACTIVITY P DIETZ 392 HOPKINS RD AMXSY TD APG MD 21005-5071
1	DIRECTOR US ARMY RESEARCH LAB AMSRL OP AP L APG MD 21005-5066
105	DIR USARL AMSRL CI AMSRL CI H W STUREK AMSRL CI S A MARK AMSRL CS IO FI M ADAMSON AMSRL SL B J SMITH AMSRL SL BA AMSRL SL BL D BELY R HENRY AMSRL SL BG AMSRL SL I AMSRL WM E SCHMIDT AMSRL WM B A HORST AMSRL WM BA F BRANDON

NO. OF COPIES ORGANIZATION

ABERDEEN PROVING GROUND (CONT)

AMSRL WM BC
P PLOSTINS
D LYON
J NEWILL
S WILKERSON
A ZIELINSKI
AMSRL WM BD
B FORCH
R FIFER
R PESCE RODRIGUEZ
B RICE
AMSRL WM BE
C LEVERITT
D KOOKER
AMSRL WM BR
C SHOEMAKER
J BORNSTEIN
AMSRL WM M
D VIECHNICKI
G HAGNAUER
J MCCAULEY
B TANNER
AMSRL WM MA
R SHUFORD
P TOUCHET
N BECK TAN
D FLANAGAN
L GHIORSE
D HARRIS
S MCKNIGHT
P MOY
P PATTERSON
G RODRIGUEZ
A TEETS
R YIN
AMSRL WM MB
B FINK
J BENDER
T BOGETTI
R BOSSOLI
L BURTON
K BOYD
S CORNELISON
P DEHMER
R DOOLEY
W DRYSDALE
G GAZONAS
S GHIORSE
D GRANVILLE

NO. OF COPIES ORGANIZATION

ABERDEEN PROVING GROUND (CONT)

D HOPKINS
C HOPPEL
D HENRY
R KASTE
M KLUSEWITZ
M LEADORE
R LIEB
E RIGAS
J SANDS
D SPAGNUOLO
W SPURGEON
J TZENG
E WETZEL
A FRYDMAN
AMRSL WM MC
J BEATTY
E CHIN
J MONTGOMERY
A WERECZCAK
J LASALVIA
J WELLS
AMSRL WM MD
W ROY
S WALSH
AMSRL WM T
B BURNS
AMSRL WM TA
W GILLICH
T HAVEL
J RUNYEON
M BURKINS
E HORWATH
B GOOCH
W BRUCHEY
AMSRL WM TC
R COATES
AMSRL WM TD
A DAS GUPTA
T HADUCH
T MOYNIHAN
F GREGORY
A RAJENDRAN
M RAFTENBERG
M BOTELER
T WEERASOORIYA
D DANDEKAR
A DIETRICH

NO. OF COPIES	ORGANIZATION

ABERDEEN PROVING GROUND (CONT)

AMSRL WM TE
A NIILER
J POWELL
AMSRL SS SD
H WALLACE
AMSRL SS SE R
R CHASE
AMSRL SS SE DS
R REYZER
R ATKINSON
AMSRL SE L
R WEINRAUB
J DESMOND
D WOODBURY

NO. OF COPIES	ORGANIZATION
1	LTD R MARTIN MERL TAMWORTH RD HERTFORD SG13 7DG UK
1	SMC SCOTLAND P W LAY DERA ROSYTH ROSYTH ROYAL DOCKYARD DUNFERMLINE FIFE KY 11 2XR UK
1	CIVIL AVIATION ADMINSTRATION T GOTTESMAN PO BOX 8 BEN GURION INTERNL AIRPORT LOD 70150 ISRAEL
1	AEROSPATIALE S ANDRE A BTE CC RTE MD132 316 ROUTE DE BAYONNE TOULOUSE 31060 FRANCE
3	DRA FORT HALSTEAD P N JONES M HINTON SEVEN OAKS KENT TN 147BP UK
1	DEFENSE RESEARCH ESTAB VALCARTIER F LESAGE COURCELETTE QUEBEC COA IRO CANADA
1	SWISS FEDERAL ARMAMENTS WKS W LANZ ALLMENDSTRASSE 86 3602 THUN SWITZERLAND
1	DYNAMEC RESEARCH AB AKE PERSSON BOX 201 SE 151 23 SODERTALJE SWEDEN

NO. OF COPIES	ORGANIZATION
1	ISRAEL INST OF TECHNOLOGY S BODNER FACULTY OF MECHANICAL ENGR HAIFA 3200 ISRAEL
1	DSTO MATERIALS RESEARCH LAB NAVAL PLATFORM VULNERABILITY SHIP STRUCTURES & MTRLS DIV N BURMAN PO BOX 50 ASCOT VALE VICTORIA AUSTRALIA 3032
1	ECOLE ROYAL MILITAIRE E CELENS AVE DE LA RENAISSANCE 30 1040 BRUXELLE BELGIQUE
1	DEF RES ESTABLISHMENT VALCARTIER A DUPUIS 2459 BOULEVARD PIE XI NORTH VALCARTIER QUEBEC CANADA PO BOX 8800 COURCELETTE GOA IRO QUEBEC CANADA
1	INSTITUT FRANCO ALLEMAND DE RECHERCHES DE SAINT LOUIS DE M GIRAUD 5 RUE DU GENERAL CASSAGNOU BOITE POSTALE 34 F 68301 SAINT LOUIS CEDEX FRANCE
1	ECOLE POLYTECH J MANSON DMX LTC CH 1015 LAUSANNE SWITZERLAND

NO. OF COPIES	ORGANIZATION
1	TNO PRINS MAURITS LABORATORY R IJSSELSTEIN LANGE KLEIWEG 137 PO BOX 45 2280 AA RIJSWIJK THE NETHERLANDS
2	FOA NATL DEFENSE RESEARCH ESTAB DIR DEPT OF WEAPONS & PROTECTION B JANZON R HOLMLIN S 172 90 STOCKHOLM SWEDEN
2	DEFENSE TECH & PROC AGENCY GROUND I CREWTHER GENERAL HERZOG HAUS 3602 THUN SWITZERLAND
1	MINISTRY OF DEFENCE RAFAEL ARMAMENT DEVELOPMENT AUTH M MAYSELESS PO BOX 2250 HAIFA 31021 ISRAEL
1	TNO DEFENSE RESEARCH I H PASMAN POSTBUS 6006 2600 JA DELFT THE NETHERLANDS
1	B HIRSCH TACHKEMONY ST 6 NETAMUA 42611 ISRAEL
1	DEUTSCHE AEROSPACE AG DYNAMICS SYSTEMS M HELD PO BOX 1340 D 86523 SCHROBENHAUSEN GERMANY

REPORT DOCUMENTATION PAGE

Form Approved
OMB No. 0704-0188

1. AGENCY USE ONLY *(Leave blank)*	2. REPORT DATE	3. REPORT TYPE AND DATES COVERED
	May 2001	Final, October 1999 - May 2000

4. TITLE AND SUBTITLE
Experimental Validation of a Closed-Form Fluid Flow Model for Vacuum-Assisted Resin-Transfer Molding

5. FUNDING NUMBERS
AH42

6. AUTHOR(S)
Bruce K. Fink, Roopesh Mathur,* Dirk Heider,* Christian Hoffman,*
John W. Gillespie, Jr.,* and Suresh G. Advani*

7. PERFORMING ORGANIZATION NAME(S) AND ADDRESS(ES)
U.S. Army Research Laboratory
ATTN: AMSRL-WM-MB
Aberdeen Proving Ground, MD 21005-5069

8. PERFORMING ORGANIZATION REPORT NUMBER
ARL-TR-2495

9. SPONSORING/MONITORING AGENCY NAMES(S) AND ADDRESS(ES)

10.SPONSORING/MONITORING AGENCY REPORT NUMBER

11. SUPPLEMENTARY NOTES
*University of Delaware, Newark, DE 19716

12a. DISTRIBUTION/AVAILABILITY STATEMENT
Approved for public release; distribution is unlimited.

12b. DISTRIBUTION CODE

13. ABSTRACT *(Maximum 200 words)*

Through-thickness measurements were recorded to experimentally investigate the through-thickness flow and to validate a closed-form solution of the resin flow during the vacuum-assisted resin-transfer molding (VARTM) process. During the VARTM process, a highly permeable distribution medium is incorporated into the preform as a surface layer, and resin is infused into the mold, under vacuum. During infusion, the resin flows preferentially across the surface and simultaneously through the thickness of the preform, giving rise to a three-dimensional flow front. The time to fill the mold and the shape of the flow front are critical for the optimal manufacture of large composite parts. An analytical model predicts the flow times and flow-front shapes as a function of the properties of the preform, distribution media, and resin. It was found that the flow-front profile reaches a steady state shape that is parabolic in shape and the length of the region saturated by resin is proportional to the square root of the time elapsed. Experimental measurements of the flow front in the process were carried out using embedded sensors to detect the flow of resin through the thickness of the preform layer and the progression of flow along the length of the part. The time to fill the part, the length of flow front, and its shape show good agreement between experiments and the analytical model. The experimental study demonstrates the need for control and optimization of resin injection during the manufacture of large parts by VARTM.

14. SUBJECT TERMS
composite material, vacuum-assisted resin-transfer molding, resin flow, sensors

15. NUMBER OF PAGES
46

16. PRICE CODE

17. SECURITY CLASSIFICATION OF REPORT	18. SECURITY CLASSIFICATION OF THIS PAGE	19. SECURITY CLASSIFICATION OF ABSTRACT	20. LIMITATION OF ABSTRACT
UNCLASSIFIED	UNCLASSIFIED	UNCLASSIFIED	UL

NSN 7540-01-280-5500

Standard Form 298 (Rev. 2-89)
Prescribed by ANSI Std. 239-18 298-102

INTENTIONALLY LEFT BLANK.

USER EVALUATION SHEET/CHANGE OF ADDRESS

This Laboratory undertakes a continuing effort to improve the quality of the reports it publishes. Your comments/answers to the items/questions below will aid us in our efforts.

1. ARL Report Number/Author ARL-TR-2495 (Fink) ____ Date of Report May 2001 ____

2. Date Report Received ____

3. Does this report satisfy a need? (Comment on purpose, related project, or other area of interest for which the report will be used.) ____

4. Specifically, how is the report being used? (Information source, design data, procedure, source of ideas, etc.) ____

5. Has the information in this report led to any quantitative savings as far as man-hours or dollars saved, operating costs avoided, or efficiencies achieved, etc? If so, please elaborate. ____

6. General Comments. What do you think should be changed to improve future reports? (Indicate changes to organization, technical content, format, etc.) ____

CURRENT ADDRESS

	Organization	
	Name	E-mail Name
	Street or P.O. Box No.	
	City, State, Zip Code	

7. If indicating a Change of Address or Address Correction, please provide the Current or Correct address above and the Old or Incorrect address below.

OLD ADDRESS

	Organization
	Name
	Street or P.O. Box No.
	City, State, Zip Code

(Remove this sheet, fold as indicated, tape closed, and mail.)

(DO NOT STAPLE)

DEPARTMENT OF THE ARMY

OFFICIAL BUSINESS

BUSINESS REPLY MAIL
FIRST CLASS PERMIT NO 0001,APG,MD

POSTAGE WILL BE PAID BY ADDRESSEE

DIRECTOR
US ARMY RESEARCH LABORATORY
ATTN AMSRL WM MB
ABERDEEN PROVING GROUND MD 21005-5069

NO POSTAGE
NECESSARY
IF MAILED
IN THE
UNITED STATES